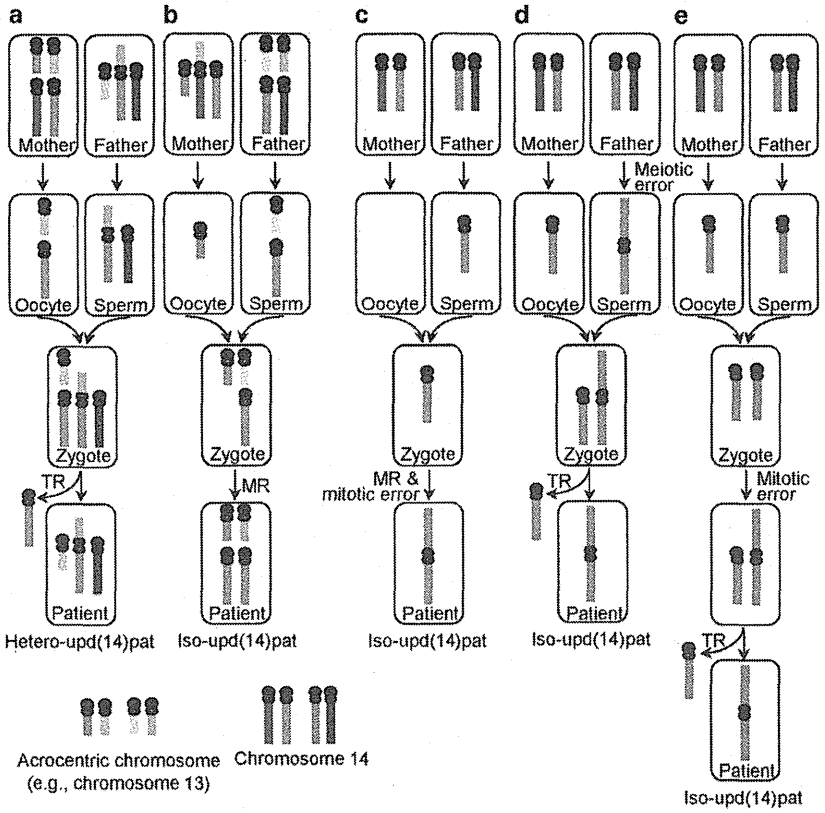

Figure 4 Schematic representation of the generation of upd(14)pat in patients or parents with Robertsonian translocation or i(14q). MR, monosomy rescue; TR, trisomy rescue; upd(14)pat, paternal uniparental disomy 14. **(a)** Hetero-upd(14)pat mediated by paternal Robertsonian translocation and post-zygotic TR. **(b)** Iso-upd(14)pat mediated by maternal Robertsonian translocation and post-zygotic MR. **(c)** Iso-upd(14)pat generated by concomitant occurrence of post-zygotic MR and isochromosome formation. **(d)** Iso-upd(14)pat generated by sequential occurrence of meiotic isochromosome formation and post-zygotic TR. **(e)** Iso-upd(14)pat generated by sequential occurrence of mitotic isochromosome formation and TR.

could occur as a *de novo* event. This indicates the production of TR-mediated upd(14)pat in these patients (Figure 4a). Here, it appears worth pointing out that a maternal Robertsonian translocation could be a risk factor for iso-upd(14)pat, because it constitutes a predisposing factor for the production of a nullisomic oocyte and resultant monosomic zygote that could be subject to MR for a paternally derived chromosome 14 (Figure 4b). However, a maternal Robertsonian translocation has not been found to date, probably because parental karyotyping has not been performed in patients with normal karyotype. In contrast, the i(14q) chromosomes with full iso-upd(14)pat in five non-Japanese patients were formed as a *de novo* event.[14–16,54,55] It is likely that the i(14q) chromosome is generated by MR in association with isochromosome formation (centromeric misdivision or U-type sister chromatid exchange) during mitosis, or by TR after isochromosome formation during meiosis or mitosis (Figures 4c–e).[49,56,57] In addition, i(14q) chromosome with hetero-upd(14)pat could be produced by U-type exchange between non-sister chromatids during meiosis.[56]

DIAGNOSTIC AND THERAPEUTIC IMPLICATIONS

Clinical diagnostic implications

The facial gestalt and the increased coat-hanger angle are mandatory for the clinical diagnosis of KOS, and the decreased M/W ratios also constitute a diagnostic indication in infancy.[10] Furthermore, when several characteristic features appear in association with the pathognomonic features, this confirms the diagnosis of KOS. Differential diagnosis includes Beckwith–Wiedemann syndrome and androgenetic mosaicism.[22,23]

Molecular diagnostic implications

The flowchart of molecular diagnosis is shown in Figure 5. As all the patients with KOS identified to date have hypermethylation of the IG-DMR and/or the *MEG3*-DMR, methylation patterns of the two DMRs should be analyzed as the first step. When hypermethylation is found for either of the two DMRs of maternal origin, this confirms the diagnosis of KOS. When hypermethylation is absent, clinical diagnosis should be reconsidered. However, it would be suggested to examine a possible deletion involving *RTL1as* but not the DMRs, or a possible mutation of *RTL1*/*RTL1as*, because loss of *RTL1as*, gain-of-function mutation of *RTL1* and loss-of-function mutation of *RTL1as* could lead to excessive *RTL1* expression. In addition, there might be microdeletions affecting *MEG3*, *MEG8*, *snoRNAs* and/or *miRNAs* but not the DMRs.

If the diagnosis of KOS is confirmed, upd(14)pat should be examined as the second step. When upd(14)pat is identified, karyotyping is recommended to examine the possibility of Robertsonian translocation or i(14q) chromosome. If the patient has such an abnormal chromosome, a recurrent risk of KOS should be considered.

When upd(14)pat is excluded, possible deletion of the IG-DMR and/or the *MEG3*-DMR should be investigated. This permits the molecular diagnosis of an epimutation when no deletion is detected

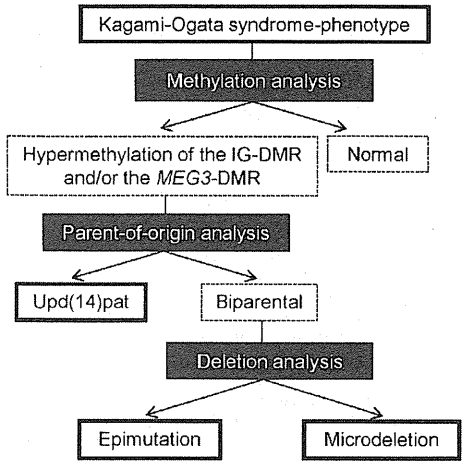

Figure 5 Molecular diagnostic flowchart. Methylation analysis is performed by combined bisulfite restriction analysis, bisulfite sequencing, multiple ligation probe amplification (MLPA) using SALSA MLPA kit ME032 UPD7/UPD14 (MRC-Holland, Amsterdam, The Netherlands) or pyrosequencing. Parent-of-origin analysis is carried out by microsatellite analysis or single-nucleotide polymorphism (SNP) array. Deletion analysis is performed by MLPA, fluorescence *in situ* hybridization or array comparative genomic hybridization. Methylation and deletion analyses need DNA samples of patients alone, whereas parent-of-origin analysis requires DNA samples of patients and their parents. MLPA is utilized for deletion analysis and methylation analysis before and after digestion of the genomic DNA samples with a methylation-sensitive restriction enzyme *Hha*I, respectively.

and that of a microdeletion when a deletion is delineated. If a deletion is identified, it is recommended to examine whether the deletion is formed as a *de novo* event or derived from the mother. In the latter case, there is a 50% recurrence risk of KOS.

Management

The management for KOS remains symptomatic, including mechanical ventilation, tracheostomy, tube feeding, surgical operation for omphalocele and supportive therapy for developmental delay. In this regard, our thorough survey data in 34 Japanese patients are summarized as follows: (1) mechanical ventilation was required by 32 patients, and was discontinued during infancy in 22 patients, with a median duration of 1 month (range, 0.1–17 months); (2) tracheostomy was performed in approximately one-third of patients; (3) tube feeding was necessary in all but a single patient, and was discontinued in 16 patients, with a median period of ~7.5 months (range, 0.1–89 months); (4) developmental delay was invariably present in 26 patients examined for developmental status, with the median developmental/intellectual quotient of 55 (range, 29–70); and (5) gross motor development was also almost invariably delayed, with head control being achieved at ~7 months (range, 3–14 months), sitting without support at ~12 months (range, 8–27 months) and walking without support at 25.5 months (range, 20–90 months) (except for a single 3-year-old patient who showed head control at 33 months of age because of severe hypotonia) (for the detailed data of individual patient, see Kagami *et al.*[10]). In addition, periodical screenings for hepatoblastoma are recommended, including serum α-fetoprotein measurement and abdominal ultrasonography.

It is worth emphasizing that patients with KOS become free from mechanical ventilation, tracheostomy and tube feeding, and there is no report of death at ≥4 years of age.[10] According to our survey, all patients go to school by themselves and get on their daily lives from childhood, although they have developmental delay. Explaining such a prognosis to parents when their affected child is in infancy and under intensive management is expected to reduce parents' anxiety and to facilitate the attachment formation between parents and the patient.

CONCLUSION

We reviewed current knowledge about KOS. Although several issues remain to be clarified, significant progress has been made for the clarification of clinical findings and underlying (epi)genetic factors. We conclude that KOS is a clinically recognizable upd(14)pat and related disorder affecting the maternally derived chromosome 14q32.2 imprinted region.

CONFLICT OF INTEREST

The authors declare no conflict of interest.

ACKNOWLEDGEMENTS

We thank Ms Emma Barber for her editorial assistance. This work was supported by Grants-in-Aid for Scientific Research (A) (25253023) and Research (B) (23390083) from the Japan Society for the Promotion of Science (JSPS), by Grants for Health Research on Children, Youth, and Families (H25-001) and for Research on Intractable Diseases (H22-161) from the Ministry of Health, Labor and Welfare (MHLW), by Grants from the National Center for Child Health and Development (23A-1, 25-10), by Grant from Takeda Science Foundation and by the Grant from the Japan Agency for Medical Research and Development (AMED) (H27-141).

1 da Rocha, S. T., Edwards, C. A., Ito, M., Ogata, T. & Ferguson-Smith, A. C. Genomic imprinting at the mammalian Dlk1-Dio3 domain. *Trends Genet.* **24**, 306–316 (2008).
2 Kagami, M., Sekita, Y., Nishimura, G., Irie, M., Kato, F., Okada, M. *et al.* Deletions and epimutations affecting the human 14q32.2 imprinted region in individuals with paternal and maternal upd(14)-like phenotypes. *Nat. Genet.* **40**, 237–242 (2008).
3 Hoffmann, K. & Heller, R. Uniparental disomies 7 and 14. *Best Pract. Res. Clin. Endocrinol. Metab.* **25**, 77–100 (2011).
4 Kagami, M., O'Sullivan, M. J., Green, A. J., Watabe, Y., Arisaka, O., Masawa, N. *et al.* The IG-DMR and the MEG3-DMR at human chromosome 14q32.2: hierarchical interaction and distinct functional properties as imprinting control centers. *PLoS Genet.* **6**, e1000992 (2010).
5 Beygo, J., Elbracht, M., de Groot, K., Begemann, M., Kanber, D., Platzer, K. *et al.* Novel deletions affecting the MEG3-DMR provide further evidence for a hierarchical regulation of imprinting in 14q32. *Eur. J. Hum. Genet.* **23**, 180–188 (2014).
6 Temple, I. K., Shrubb, V., Lever, M., Bullman, H. & Mackay, D. J. Isolated imprinting mutation of the DLK1/GTL2 locus associated with a clinical presentation of maternal uniparental disomy of chromosome 14. *J. Med. Genet.* **44**, 637–640 (2007).
7 Hosoki, K., Ogata, T., Kagami, M., Tanaka, T. & Saitoh, S. Epimutation (hypomethylation) affecting the chromosome 14q32.2 imprinted region in a girl with upd(14)mat-like phenotype. *Eur. J. Hum. Genet.* **16**, 1019–1023 (2008).
8 Buiting, K., Kanber, D., Martín-Subero, J. I., Lieb, W., Terhal, P., Albrecht, B. *et al.* Clinical features of maternal uniparental disomy 14 in patients with an epimutation and a deletion of the imprinted DLK1/GTL2 gene cluster. *Hum. Mutat.* **29**, 1141–1146 (2008).
9 Zechner, U., Kohlschmidt, N., Rittner, G., Damatova, N., Beyer, V., Haaf, T. *et al.* Epimutation at human chromosome 14q32.2 in a boy with a upd(14)mat-like clinical phenotype. *Clin. Genet.* **75**, 251–258 (2009).
10 Kagami, M., Kurosawa, K., Miyazaki, O., Ishino, F., Matsuoka, K. & Ogata, T. Comprehensive clinical studies in 34 patients with molecularly defined UPD(14)pat and related conditions (Kagami-Ogata syndrome). *Eur. J. Hum. Genet* (e-pub ahead of print 18 February 2015; doi: 10.1038/ejhg.2015.13).
11 Ioannides, Y., Lokulo-Sodipe, K., Mackay, D. J., Davies, J. H. & Temple, I. K. Temple syndrome: improving the recognition of an underdiagnosed chromosome 14 imprinting disorder: an analysis of 51 published cases. *J. Med. Genet.* **51**, 495–501 (2014).
12 Wang, J. C., Passage, M. B., Yen, P. H., Shapiro, L. J. & Mohandas, T. K. Uniparental heterodisomy for chromosome 14 in a phenotypically abnormal familial balanced 13/14 Robertsonian translocation carrier. *Am. J. Hum. Genet.* **48**, 1069–1074 (1991).
13 Cotter, P. D., Kaffe, S., McCurdy, L. D., Jhaveri, M., Willner, J. P. & Hirschhorn, K. Paternal uniparental disomy for chromosome 14: a case report and review. *Am. J. Med. Genet.* **70**, 74–79 (1997).
14 Papenhausen, P. R., Mueller, O. T., Sutcliffe, M., Diamond, T. M., Kousseff, B. G. & Johnson, V. P. Uniparental isodisomy of chromosome 14 in two cases: an abnormal child and a normal adult. *Am. J. Med. Genet.* **59**, 271–275 (1995).

15 Walter, C. A., Shaffer, L. G., Kaye, C. I., Huff, R. W., Ghidoni, P. D., McCaskill, C. *et al.* Short-limb dwarfism and hypertrophic cardiomyopathy in a patient with paternal isodisomy 14: 45,XY,idic(14)(p11). *Am. J. Med. Genet.* **65**, 259–265 (1996).
16 Stevenson, D. A., Brothman, A. R., Chen, Z., Bayrak-Toydemir, P. & Longo, N. Paternal uniparental disomy of chromosome 14: confirmation of a clinically-recognizable phenotype. *Am. J. Med. Genet. A* **130A**, 88–91 (2004).
17 Kurosawa, K., Sasaki, H., Sato, Y., Yamanaka, M., Shimizu, M., Ito, Y. *et al.* Paternal UPD14 is responsible for a distinctive malformation complex. *Am. J. Med. Genet.* **110**, 268–272 (2002).
18 Coveler, K. J., Yang, S. P., Sutton, R., Milstein, J. M., Wu, Y. Q., Bois, K. D. *et al.* A case of segmental paternal isodisomy of chromosome 14. *Hum. Genet.* **110**, 251–256 (2002).
19 Curtis, L., Antonelli, E., Vial, Y., Rimensberger, P., Le Merrer, M., Hinard, C. *et al.* Prenatal diagnostic indicators of paternal uniparental disomy 14. *Prenat. Diagn.* **26**, 662–666 (2006).
20 Mattes, J., Whitehead, B., Liehr, T., Wilkinson, I., Bear, J., Fagan, K. *et al.* Paternal uniparental isodisomy for chromosome 14 with mosaicism for a supernumerary marker chromosome 14. *Am. J. Med. Genet. A* **143A**, 2165–2171 (2007).
21 Irving, M. D., Buiting, K., Kanber, D., Donaghue, C., Schulz, R., Offiah, A. *et al.* Segmental paternal uniparental disomy (patUPD) of 14q32 with abnormal methylation elicits the characteristic features of complete patUPD14. *Am. J. Med. Genet. A* **152A**, 1942–1950 (2010).
22 Weksberg, R., Shuman, C. & Beckwith, J. B. Beckwith-Wiedemann syndrome. *Eur. J. Hum. Genet.* **18**, 8–14 (2010).
23 Yamazawa, K., Nakabayashi, K., Matsuoka, K., Masubara, K., Hata, K., Horikawa, R. *et al.* Androgenetic/biparental mosaicism in a girl with Beckwith-Wiedemann syndrome-like and upd(14)pat-like phenotypes. *J. Hum. Genet.* **56**, 91–93 (2011).
24 Kohrle, J. Thyroid hormone transporters in health and disease: advances in thyroid hormone deiodination. *Best Pract. Res. Clin. Endocrinol. Metab* **21**, 173–191 (2007).
25 Wallace, C., Smyth, D. J., Maisuria-Armer, M., Walker, N. M., Todd, J. A. & Clayton, D. G. The imprinted DLK1-MEG3 gene region on chromosome 14q32.2 alters susceptibility to type 1 diabetes. *Nat. Genet.* **42**, 68–71 (2010).
26 Kameswaran, V., Bramswig, N. C., McKenna, L. B., Penn, M., Schug, J., Hand, N. J. *et al.* Epigenetic regulation of the DLK1-MEG3 microRNA cluster in human type 2 diabetic islets. *Cell Metab.* **19**, 135–145 (2014).
27 Kagami, M., Matsuoka, K., Nagai, T., Yamanaka, M., Kurosawa, K., Suzumori, N. *et al.* Paternal uniparental disomy 14 and related disorders: placental gene expression analyses and histological examinations. *Epigenetics* **7**, 1142–1150 (2012).
28 Murphy, S. K., Wylie, A. A., Coveler, K. J., Cotter, P. D., Papenhausen, P. R., Sutton, V. R. *et al.* Epigenetic detection of human chromosome 14 uniparental disomy. *Hum. Genet.* **22**, 92–97 (2003).
29 Nowak, K., Stein, G., Powell, E., He, L. M., Naik, S., Morris, J. *et al.* Establishment of paternal allele-specific DNA methylation at the imprinted mouse Gtl2 locus. *Epigenetics* **6**, 1012–1020 (2011).
30 Kagami, M., Kato, F., Matsubara, K., Sato, T., Nishimura, G. & Ogata, T. Relative frequency of underlying genetic causes for the development of UPD(14)pat-like phenotype. *Eur. J. Hum. Genet.* **20**, 928–932 (2012).
31 Tierling, S., Dalbert, S., Schoppenhorst, S., Tsai, C. E., Oliger, S., Ferguson-Smith, A. C. *et al.* High-resolution map and imprinting analysis of the Gtl2-Dnchc1 domain on mouse chromosome 12. *Genomics* **87**, 225–235 (2007).
32 Benetatos, L., Hatzimichael, E., Londin, E., Vartholomatos, G., Loher, P., Rigoutsos, I. *et al.* The microRNAs within the DLK1-DIO3 genomic region: involvement in disease pathogenesis. *Cell Mol Life Sci.* **70**, 795–814 (2013).
33 Kota, S. K., Llères, D., Bouschet, T., Hirasawa, R., Marchand, A., Begon-Pescia, C. *et al.* ICR noncoding RNA expression controls imprinting and DNA replication at the Dlk1-Dio3 domain. *Dev. Cell* **31**, 19–33 (2014).
34 Kim, T. K., Hemberg, M., Gray, J. M., Costa, A. M., Bear, D. M., Wu, J. *et al.* Widespread transcription at neuronal activity-regulated enhancers. *Nature* **465**, 182–187 (2010).
35 Wang, D., Garcia-Bassets, I., Benner, C., Li, W., Su, X., Zhou, Y. *et al.* Reprogramming transcription by distinct classes of enhancers functionally defined by eRNA. *Nature* **474**, 390–394 (2011).
36 Shin, S., Han, J.Y. & Lee, K. Cloning of avian Delta-like 1 homolog gene: the biallelic expression of Delta-like 1 homolog in avian species. *Poult Sci.* **89**, 948–955 (2010).
37 Glazov, E.A., McWilliam, S., Barris, W.C. & Dalrymple, B.P. Origin, evolution, and biological role of miRNA cluster in DLK-DIO3 genomic region in placental mammals. *Mol. Biol. Evol.* **25**, 939–948 (2008).
38 Rosa, A. L., Wu, Y. Q., Kwabi-Addo, B., Coveler, K. J., Reid. Sutton, V. & Shaffer, L. G. Allele-specific methylation of a functional CTCF binding site upstream of MEG3 in the human imprinted domain of 14q32. *Chromosome Res.* **13**, 809–818 (2005).
39 Carr, M. S., Yevtodiyenko, A., Schmidt, C. L. & Schmidt, J. V. Allele-specific histone modifications regulate expression of the Dlk1-Gtl2 imprinted domain. *Genomics* **89**, 280–290 (2007).
40 Wan, L. B., Pan, H., Hannenhalli, S., Cheng, Y., Ma, J., Fedoriw, A. *et al.* Maternal depletion of CTCF reveals multiple functions during oocyte and preimplantation embryo development. *Development* **135**, 2729–2738 (2008).
41 McMurray, E. N. & Schmidt, J. V. Identification of imprinting regulators at the Meg3 differentially methylated region. *Genomics* **100**, 184–194 (2012).
42 Stelzer, Y., Sagi, I., Yanuka, O., Eiges, R. & Benvenisty, N. The noncoding RNA lPW regulates the imprinted DLK1-DIO3 locus in an induced pluripotent stem cell model of Prader-Willi syndrome. *Nat Genet.* **46**, 551–557 (2014).
43 Seitz, H., Youngson, N., Lin, S. P., Dalbert, S., Paulsen, M., Bachellerie, J. P. *et al.* Imprinted microRNA genes transcribed antisense to a reciprocally imprinted retrotransposon-like gene. *Nat. Genet.* **34**, 261–262 (2003).
44 Sekita, Y., Wagatsuma, H., Nakamura, K., Ono, R., Kagami, M., Wakisaka, N. *et al.* Role of retrotransposon-derived imprinted gene, Rtl1, in the feto-maternal interface of mouse placenta. *Nat. Genet.* **40**, 243–248 (2008).
45 Brandt, J., Schrauth, S., Veith, A. M., Froschauer, A., Haneke, T., Schultheis, C. *et al.* Transposable elements as a source of genetic innovation: expression and evolution of a family of retrotransposon-derived neogenes in mammals. *Gene* **345**, 101–111 (2005).
46 da Rocha, S.T., Tevendale, M., Knowles, E., Takada, S., Watkins, M. & Ferguson-Smith, A. C. Restricted co-expression of Dlk1 and the reciprocally imprinted non-coding RNA, Gtl2: implications for cis-acting control. *Dev. Biol.* **306**, 810–823 (2007).
47 Sahoo, T., del Gaudio, D., German, J. R., Shinawi, M., Peters, S. U., Person, R. E. *et al.* Prader-Willi phenotype caused by paternal deficiency for the HBII-85 C/D box small nucleolar RNA cluster. *Nat. Genet.* **40**, 719–721 (2008).
48 Cunningham, F. G., Leveno, K. J., Bloom, S. L., Spong, C. Y., Dashe, J. S., Hoffman, B. L. *et al. Williams Obstetrics* 24th edn 231–239 (McGraw-Hill Education, New York, NY, USA, 2014).
49 Berend, S. A., Horwitz, J., McCaskill, C. & Shaffer, L. G. Identification of uniparental disomy following prenatal detection of Robertsonian translocations and isochromosomes. *Am. J. Hum. Genet.* **66**, 1787–1793 (2000).
50 Ji, Y., Walkowicz, M. J., Buiting, K., Johnson, D. K., Tarvin, R. E., Rinchik, EM. *et al.* The ancestral gene for transcribed, low-copy repeats in the Prader-Willi/Angelman region encodes a large protein implicated in protein trafficking, which is deficient in mice with neuromuscular and spermiogenic abnormalities. *Hum. Mol. Genet.* **8**, 533–542 (1999).
51 Matsubara, K., Murakami, N., Nagai, T. & Ogata, T. Maternal age effect on the development of Prader-Willi syndrome resulting from upd(15)mat through meiosis 1 errors. *J. Hum. Genet.* **56**, 566–571 (2011).
52 Pellestor, F., Andreo, B., Anahory, T. & Hamamah, S. The occurrence of aneuploidy in human: lessons from the cytogenetic studies of human oocytes. *Eur. J. Med. Genet.* **49**, 103–116 (2006).
53 Yano, S., Li, L., Owen, S., Wu, S. & Tran, T. A further delineation of the uniparental disomy (UPD 14): the fifth reported liveborn case. *Am. J. Hum. Genet.* **69**, A739 (2001).
54 Klein, J., Shaffer, L., McCaskill, C., Sheerer, L., Otto, C. & Main, D. Delineation of the paternal disomy 14 syndrome: identification of a case by prenatal diagnosis. *Am. J. Hum. Genet.* **65**, A179 (1999).
55 McGowan, K. D., Weiser, J. J., Horwitz, J., Berend, S. A., McCaskill, C., Sutton, V. R. *et al.* The importance of investigating for uniparental disomy in prenatally identified balanced acrocentric rearrangements. *Prenat. Diagn.* **22**, 141–143 (2002).
56 Baumer, A., Basaran, S., Taralczak, M., Cefle, K., Ozturk, S., Palanduz, S. *et al.* Initial maternal meiotic I error leading to the formation of a maternal i(2q) and a paternal i(2p) in a healthy male. *Cytogenet. Genome. Res.* **118**, 38–41 (2007).
57 Wang, J. C., Vaccarello-Cruz, M., Ross, L., Owen, R., Pratt, V. M., Lightman, K. *et al.* Mosaic isochromosome 15q and maternal uniparental isodisomy for chromosome 15 in a patient with morbid obesity and variant PWS-like phenotype. *Am. J. Med. Genet. A* **161A**, 1695–1701 (2013).

Supplementary Information accompanies the paper on Journal of Human Genetics website (http://www.nature.com/jhg)

Endocrine (2015) 49:553–556
DOI 10.1007/s12020-014-0434-4

RESEARCH LETTER

Hypogonadotropic hypogonadism in a female patient previously diagnosed as having waardenburg syndrome due to a sox10 mutation

Yoko Izumi · Ikuma Musha · Erina Suzuki · Manami Iso · Tomoko Jinno · Reiko Horikawa · Shin Amemiya · Tsutomu Ogata · Maki Fukami · Akira Ohtake

Received: 6 June 2014 / Accepted: 19 September 2014 / Published online: 2 October 2014

Introduction

Hypogonadotropic hypogonadism (HH) is a clinically and genetically heterogeneous condition that can be associated with several additional clinical features such as anosmia, cleft palate, and hearing loss [1]. HH with anosmia is referred to as Kallmann syndrome (KS). More than 20 genes are known to underlie HH and/or KS, although mutations in these genes account for only a minor portion of the etiology of HH/KS [1–4]. In 2013, Pingault et al. identified *SOX10* mutations in seven patients with KS [5]. Furthermore, Pingault et al. found that genetic knockout of *Sox10* disrupted migration of GnRH cells in murine fetuses [5]. Subsequently, Vaaralahti et al. identified an additional KS patient with a *SOX10* mutation [6]. These results indicate that *SOX10* mutations constitute rare genetic causes of KS. Currently, *SOX10* is known as one of the causative genes of Waardenburg syndrome (WS), a rare genetic disorder characterized by hearing loss and hypopigmentation in the skin, hair, and eye [7]. Indeed, hearing impairment with or without gray/white hair was found in most of the KS cases reported by Pingault et al. and Vaaralahti et al. [5, 6]. However, detailed clinical assessment of the *SOX10* mutation-positive patients and functional assays of the *SOX10* mutants remain fragmentary. Thus, genetic links between HH/KS and WS have not been fully established. Here, we performed molecular and clinical analyses of a previously reported patient with WS due to a frameshift mutation in *SOX10*.

Patient

The patient was first described in 2008 as an infant with WS-type 2 (WS without dystopia canthorum) [8]. Shortly after birth, she presented with hypopigmented irides and a

Yoko Izumi, Ikuma Musha, and Erina Suzuki contributed equally to this work.

Electronic supplementary material The online version of this article (doi:10.1007/s12020-014-0434-4) contains supplementary material, which is available to authorized users.

Y. Izumi · E. Suzuki · M. Iso · T. Jinno · T. Ogata · M. Fukami (✉)
Department of Molecular Endocrinology, National Research Institute for Child Health and Development, 2-10-1 Ohkura, Setagaya, Tokyo 157-8535, Japan
e-mail: fukami-m@ncchd.go.jp

Y. Izumi
Department of Obstetrics and Gynecology, Keio University School of Medicine, 35 Shinanomachi, Shinjuku, Tokyo 160-8582, Japan

I. Musha · S. Amemiya · A. Ohtake
Department of Pediatrics, Faculty of Medicine, Saitama Medical University, 38 Morohongo Moroyama-machi, Iruma-Gun, Saitama 350-0495, Japan

R. Horikawa
Department of Endocrinology and Metabolism, National Center for Child Health and Development, 2-10-1 Ohkura, Setagaya, Tokyo 157-8535, Japan

T. Ogata
Department of Pediatrics, Hamamatsu University School of Medicine, 1-20-1 Handayama, Higashi-ku, Hamamatsu, Shizuoka 431-3192, Japan

piece of white forelock. Dystopia canthorum, broad nasal root, limb anomaly, and Hirschsprung disease were absent. Ophthalmologic examinations revealed bilateral ocular albinism with hypopigmented fundus and hypochromic iris. Auditory brainstem response indicated bilateral sensorineural deafness. The patient underwent cochlear implantation at 2.6 years of age. Direct sequence analysis of WS causative genes (*SOX10, PAX3*, *MITF* and *SNAI2*) identified a heterozygous mutation in *SOX10* (c.506delC, p.P169fsX117) and excluded mutations in the other genes [8]. Until nine years of age, her growth followed the −1.0 standard deviation (SD) growth curve of Japanese female population. Thereafter, the SD scores for height and height velocity gradually decreased.

At 12.9 years of age, she revisited our clinic because of delayed puberty. Physical examination revealed mild short stature (−2.1 SD) and a lack of pubertal signs (breast and pubic hair, Tanner stage 1) (Figure S1). A smell test using intravenous injection of combined vitamins (Alinamin, Takeda Pharmaceutical Co. Ltd., Japan) [9] induced no response. Other standard smell tests such as UPSIT were not performed. Her bone age was delayed (~11 years of age). Endocrine studies revealed a low level of estradiol (E_2), together with apparently normal gonadotropin levels at the baseline and after GnRH stimulation (Table 1). The blood values of other hormones were grossly normal; whereas the TSH response to TRH was blunted, normal levels of thyroid hormones suggested preserved thyroid function [10, 11]. Low E_2 levels and normal gonadotropin levels were also observed in examinations performed at 13.8 and 14.1 years of age (Table 1). Brain magnetic resonance imaging (MRI) was not performed, because her cochlear implants contained magnetic components. From 14.1 years of age, she received E_2 supplementation therapy, which successfully induced breast budding and improved height growth (Figure S1). To confirm the genetic basis of HH in this patient, we performed further molecular analyses.

Methods

This study was approved by the Institutional Review Board Committee at the National Center for Child Health and Development and performed after obtaining informed consent. Mutation screening was carried out for the coding regions of 20 causative genes for HH/KS: *CHD7*, *FGF8*, *FGFR1*, *FSHB*, *GNRH1*, *GNRHR*, *HS6ST1*, *KAL1*, *KISS1*, *KISS1R*, *LEP*, *LEPR*, *LHB*, *NELF*, *PROK2*, *PROKR2*, *SEMA3A*, *TAC3*, *TACR3*, and *WDR11* [2, 4]. Nucleotide alterations were determined by the Haloplex system (Agilent Technologies, Palo Alto, CA, USA) on a MiSeq sequencer (Illumina, San Diego, CA, USA). Genome-wide copy-number analysis was performed by oligoarray-based comparative genomic hybridization using an array-based catalog CGH (4 × 180 k format, catalog number G4449A; Agilent Technologies).

In vitro reporter assays for the *SOX10* mutation were carried out by a previously reported method with slight modifications [12, 13]. An expression vector for wildtype *SOX10* was purchased from Kazusa DNA Research Institute (Kisarazu, Chiba, Japan). An expression vector for the mutant *SOX10* was generated by site-directed mutagenesis. A luciferase reporter vector containing the *MITF* promoter sequence (–2253 to +97 bp) and an expression vector for *PAX3* [12, 13] were kindly provided by Dr. Bondurand and Professor Goossens. Transient transfection was performed using HEK293 cells seeded in 24-well plates (1.0×10^5 cells/well) and Lipofectamine 2000 Reagent (Life technologies, Carlsbad, CA, USA), with the expression vectors (20 ng/well or 40 ng/well), the luciferase reporter vector (10 ng/well), and a pCMV-PRL internal control vector (5 ng/well; Promega, Madison, WI, USA). As controls for the expression vectors, an empty counterpart vector (HaloTag vector, Promega) was transfected. At 48 h after transfection, the cells were harvested and subjected to luciferase analysis using the dual luciferase reporter assay system and GloMax Luminometer (Promega). Luciferase assays were also performed with co-expression of a *PAX3* expression vector (20 ng/well). These experiments were carried out in triplicate within a single experiment and the experiment was repeated four times. Statistical significance was determined by the *t* test.

To predict the pathogenicity of the *SOX10* mutation, we performed direct sequencing of *SOX10* for the samples obtained from the clinically normal parents of the patient. In this experiment, we used previously described primers [8].

Results

Mutation screening excluded mutations in other HH/KS-associated genes. Comparative genomic hybridization analysis detected no pathogenic copy-number alterations. The mutant SOX10 protein barely transactivated the *MITF* promoter and exerted no dominant-negative effect on wildtype SOX10 (Figure S2). The *SOX10* mutation was not detected in the parental samples.

Discussion

Herein, we report a female patient who developed HH. Although standard smell tests and brain MRI were not performed for the patient, the lack of response to

Table 1 Endocrine data of the patient

Hormone	Stimulus (dosage)	Patient		Reference values[a]	
		Baseline	Peak	Baseline	Peak
At 12.9 years of age					
LH (mIU/ml)	GnRH (100 μg)[b]	1.0	11.8	0.4–4.1	8.5–15.5
FSH (mIU/ml)	GnRH (100 μg)[b]	2.6	13.2	4.8–10.4	8.3–20.0
Estradiol (pg/ml)		<10		<10–144	
GH (ng/ml)	Insulin (3 U)[b]	3.74	**4.83**[c]	0.3–33.1	>6.0
GH (ng/ml)	Arginine (18 g)[d]	4.2	9.7	0.3–33.1	>6.0
Prolactin (ng/ml)	TRH (350 μg)[b]	25.2	43.1	1.2–13.2	2.4–52.8
TSH (μIU/ml)	TRH (350 μg)[b]	1.64	**5.08**	0.32–4.0	10–35
ACTH (pg/ml)	Insulin (3 U)[b]	55.8	88.4	5.2–38.8	10.4–116.4
Cortisol (μg/dl)	Insulin (3 U)[b]	25.2	29.8	3.0–12.0	6.0–36.0
IGF-1 (ng/ml)		205		206–731	
Free T_3 (pg/ml)		3.94		2.43–4.48	
Free T_4 (ng/dl)		1.05		0.98–1.90	
At 13.8 years of age					
LH (mIU/ml)	GnRH (100 μg)[b]	1.0	12.3	0.2–2.1	1.7–5.0
FSH (mIU/ml)	GnRH (100 μg)[b]	2.6	11.6	0.6–3.4	1.4–11.5
Estradiol (pg/ml)		**<10**		12–162	
At 14.1 years of age					
LH (mIU/ml)	GnRH (100 μg)[b]	0.6	10.0	0.2–2.1	1.7–5.0
FSH (mIU/ml)	GnRH (100 μg)[b]	2.5	10.5	0.6–3.4	1.4–11.5
Estradiol (pg/ml)	hMG (150 U)[e]	**<10**	430	13–174	300–1000

The conversion factors to the SI unit: LH, 1.0 (IU/liter); FSH, 1.0 (IU/liter); GH, 1.0 (μg/liter); prolactin, 43.48 (pmol/liter); TSH, 1.0 (mIU/liter); ACTH, 0.22 (pmol/liter); cortisol, 27.59 (nmol/liter), estradiol, 3.671 (pmol/liter); free T_3, 1.536 (pmol/liter); free T_4, 0.1287 (pmol/liter)

Hormone values below the reference range are boldfaced

[a] Reference values in age-matched Japanese females [10, 11]

[b] GnRH, insulin, and TRH i.v.; blood sampling at 0, 30, 60, 90, and 120 min

[c] Low GH may be due to insufficient hypoglycemic stimulation

[d] Arginine i.v.; blood sampling at 0, 30, 60, 90, and 120 min

[e] hMG i.m. for 4 consecutive days; blood sampling on days 1 and 4

intravenous injection of combined vitamins indicated impaired olfactory function. In infancy, the patient was diagnosed as having WS due to a *SOX10* mutation [8]. In the present study, we performed further molecular analysis of the patient and excluded mutations in other HH/KS-associated genes and copy-number alterations in the genome. Furthermore, we confirmed that the *SOX10* mutation is not shared by the clinically normal parents and that the mutant SOX10 has impaired transactivating activity for the *MITF* promoter. These results indicate that the phenotype of this patient results from the *SOX10* mutation. However, we cannot exclude the possibility that the patient has an additional mutation in a hitherto unknown HH/KS-causative gene, because several unidentified genes seem to underlie HH/KS [2–4]. To date, hypogonadism is known as a relatively rare complication in patients with WS due to *SOX10* mutation/deletion [14]. Furthermore, hearing loss was observed in most of the previously reported patients with KS and *SOX10* mutations [5, 6], although hypopigmentation in the eye or skin were not described in these individuals. Our data, together with the previous findings, indicate that *SOX10* mutations can lead to various developmental defects including an overlapping phenotype of HH/KS and WS. Therefore, thorough clinical evaluations including hormonal assessment should be performed for WS patients with *SOX10* mutations, because subnormal gonadotropin secretion may account for a certain fraction of such patients.

It is worth mentioning that our patient showed normal gonadotropin responses to GnRH stimulation and a normal estrogen response to human menopausal gonadotropin stimulation. Thus, hypothalamic dysfunction appears to be the primary lesion of this patient. These results are consistent with the previously proposed notion that SOX10

plays a critical role in the development of hypothalamic neurons [5]. *SOX10* mutations are likely to cause gonadotropin deficiency as a sole hormonal defect, because the levels of blood hormones except for E_2 remained grossly normal in our patient.

The results of in vitro assays suggest that *SOX10* mutations lead to the disease phenotype by haploinsufficiency rather than by dominant-negative effects. The broad phenotypic variation of *SOX10* mutation-positive patients can be explained by the notion that haploinsufficiency of developmental genes is usually associated with a wide range of penetrance and expressivity [15].

In conclusion, the present study provides evidence that *SOX10* haploinsufficiency underlies a continuum of developmental defects that includes both HH and WS. Hypothalamic dysfunction appears to be the major hormonal defect resulting from *SOX10* mutations. Further studies will clarify the prevalence and clinical characteristics of *SOX10* abnormalities.

Acknowledgments We thank Dr. Nadege Bondurand and Professor Michel Goossens for providing us the *MITF* reporter vector and the *PAX3* expression vector.

This study was supported by grants from the Ministry of Health, Labor and Welfare, and from Takeda Science Foundation, by Grants-in-Aid for Scientific Research from the Japan Society for the Promotion of Science and from the Ministry of Education, Culture, Sports, Science, and Technology, and by the Grant of National Center for Child Health and Development.

Conflict of interest All the authors declare that there is no conflict of interest.

References

1. R. Rapaport, Disorders of the gonads, in *Nelson textbook of pediatrics*, 18th edn., ed. by R.M. Kliegman, R.E. Behrman, H.B. Jenson, B.F. Stanton (Saunders, Philadelphia, 2007), pp. 2374–2403
2. L.C. Layman, The genetic basis of female reproductive disorders: etiology and clinical testing. Mol. Cell. Endocrinol. **370**(1–2), 138–148 (2013)
3. H. Miraoui, A.A. Dwyer, G.P. Sykiotis, L. Plummer, W. Chung, B. Feng, A. Beenken, J. Clarke, T.H. Pers, P. Dworzynski, K. Keefe, M. Niedziela, T. Raivio, W.F.Jr Crowley, S.B. Seminara, R. Quinton, V.A. Hughes, P. Kumanov, J. Young, M.A. Yialamas, J.E. Hall, G.V. Vliet, J.P. Chanoine, J. Rubenstein, M. Mohammadi, P.S. Tsai, Y. Sidis, K. Lage, N. Pitteloud, Mutations in FGF17, IL17RD, DUSP6, SPRY4, and FLRT3 are identified in individuals with congenital hypogonadotropic hypogonadism. Am. J. Hum. Genet. **92**(5), 725–743 (2013)
4. Y. Izumi, E. Suzuki, S. Kanzaki, S. Yatsuga, S. Kinjo, M. Igarashi, T. Maruyama, S. Sano, R. Horikawa, N. Sato, K. Nakabayashi, K. Hata, A. Umezawa, T. Ogata, Y. Yoshimura, M. Fukami, Genome-wide copy number analysis and systematic mutation screening in 58 patients with hypogonadotropic hypogonadism. Fertil. Steril. (2014). doi:10.1016/j.fertnstert.2014.06.017
5. V. Pingault, V. Bodereau, V. Baral, S. Marcos, Y. Watanabe, A. Chaoui, C. Fouveaut, C. Leroy, O. Vérier-Mine, C. Francannet, D. Dupin-Deguine, F. Archambeaud, F.J. Kurtz, J. Young, J. Bertherat, S. Marlin, M. Goossens, J.P. Hardelin, C. Dodé, N. Bondurand, Loss-of-function mutations in SOX10 cause Kallmann syndrome with deafness. Am. J. Hum. Genet. **92**(5), 707–724 (2013)
6. K. Vaaralahti, J. Tommiska, V. Tillmann, N. Liivak, J. Känsäkoski, E.M. Laitinen, T. Raivio, De novo SOX10 nonsense mutation in a patient with Kallmann syndrome and hearing loss. Pediatr. Res. (2014). doi:10.1038/pr.2014.60
7. V. Pingault, D. Ente, F. Dastot-Le Moal, M. Goossens, S. Marlin, N. Bondurand, Review and update of mutations causing Waardenburg syndrome. Hum. Mutat. **31**(4), 391–406 (2010)
8. M. Iso, M. Fukami, R. Horikawa, N. Azuma, N. Kawashiro, T. Ogata, SOX10 mutation in Waardenburg syndrome type II. Am. J. Med. Genet. A. **146A**(16), 2162–2163 (2008)
9. M. Furukawa, M. Kamide, T. Miwa, R. Umeda, Significance of intravenous olfaction test using thiamine propyldisulfide (Alinamin) in olfactometry. Auris Nasus Larynx **15**(1), 25–31 (1988)
10. T. Tanaka: Endocrine examination. In: T. Tanaka (ed.) New pocket guide of clinical standard values for children. 1st ed., 106-132. Jihou, Tokyo, (2009) [In Japanese]
11. H. Inada, T. Imamura, R. Nakajima: Assessment of pituitary function. In; H. Inada, T. Imamura, R. Nakajima (eds.) Manual of endocrine examinations of children. 2nd ed., 5-22. Medical Review, Osaka, (2002) [In Japanese]
12. N. Bondurand, V. Pingault, D.E. Goerich, N. Lemort, E. Sock, C.L. Caignec, M. Wegner, M. Goossens, Interaction among SOX10, PAX3 and MITF, three genes altered in Waardenburg syndrome. Hum. Mol. Genet. **9**(13), 1907–1917 (2000)
13. H. Zhang, H. Chen, H. Luo, J. An, L. Sun, L. Mei, C. He, L. Jiang, W. Jiang, K. Xia, J.D. Li, Y. Feng, Functional analysis of Waardenburg syndrome-associated PAX3 and SOX10 mutations: report of a dominant-negative SOX10 mutation in Waardenburg syndrome type II. Hum. Genet. **131**(3), 491–503 (2012)
14. B. Jelena, L. Christina, V. Eric, Q.R. Fabiola, Phenotypic variability in Waardenburg syndrome resulting from a 22q12.3-q13.1 microdeletion involving SOX10. Am. J. Med. Genet A. **164**(6), 1512–1519 (2014)
15. E. Fisher, P. Scambler, Human haploinsufficiency-one for sorrow, two for joy. Nat. Genet. **7**(1), 5–7 (1994)

Original Article

Sexual Development

Sex Dev 2015;9:130–135
DOI: 10.1159/000380842

Accepted: December 30, 2014
by M. Schmid
Published online: March 31, 2015

Novel Splice Site Mutation in *MAMLD1* in a Patient with Hypospadias

Maki Igarashi[a] Yuka Wada[a] Yoshiyuki Kojima[b, c] Mami Miyado[a]
Michiko Nakamura[d] Koji Muroya[e] Kentaro Mizuno[b] Yutaro Hayashi[b]
Katsuya Nonomura[d] Kenjiro Kohri[b] Tsutomu Ogata[a, f] Maki Fukami[a]

[a]Department of Molecular Endocrinology, National Research Institute for Child Health and Development, Tokyo, [b]Department of Nephro-Urology, Nagoya City University Graduate School of Medical Sciences, Nagoya, [c]Department of Urology, Fukushima Medical University School of Medicine, Fukushima, [d]Department of Renal and Genitourinary Surgery, Hokkaido University Graduate School of Medicine, Sapporo, [e]Department of Endocrinology and Metabolism, Kanagawa Children's Medical Center, Yokohama, and [f]Department of Pediatrics, Hamamatsu University School of Medicine, Hamamatsu, Japan

Key Words
Hypospadias · *MAMLD1* · Mutation · Protein · Splicing · Translation

Abstract
MAMLD1 is a causative gene for disorders of sex development. Several *MAMLD1* mutations have been shown to cause hypospadias by generating dysfunctional proteins and/or unstable mRNAs. Here, we identified an intronic mutation of *MAMLD1* (g.IVS4−2A>G) in 1 of 180 hypospadias patients. RT-PCR of the patient's skin sample showed normal expression of full-length *MAMLD1* and markedly reduced expression of a known splice variant lacking exon 4. A hitherto unreported splice variant that lacks exon 5 was similarly identified in samples of the patient and control individuals. The full-length transcript of the patient contained mutant mRNA lacking the first 10 nucleotides of exon 5 (c.1822_1831delACTCATGTAG, p.K609fsX1070). In vitro assays using cells expressing the full-length wild-type and mutant proteins revealed reduced expression of the mutant. The expression of the wild-type and mutant MAMLD1 showed parallel changes upon treatment with a proteasome inhibitor and a translation inhibitor. The mutant-expressing cells exerted low transactivation activity for the *Hes3* promoter, which reflected limited expression of the mutant protein. These results imply that the pathogenic events resulting from *MAMLD1* mutations include splice errors. Furthermore, this study raises the possibility of translation failure of MAMLD1 mutants, which deserves further investigation.

MAMLD1 (NM_001177465) on Xq28 is a causative gene for 46,XY disorders of sex development (DSD) [Fukami et al., 2006]. The major clinical feature of patients with *MAMLD1* mutations is hypospadias [Fukami et al., 2006]. Previous studies have shown that MAMLD1 transactivates the promoter of the non-canonical Notch target *Hes3* and enhances expression of multiple genes in murine fetal Leydig cells [Fukami et al., 2008; Miyado et al., 2012]. Human *MAMLD1* comprises at least 7 exons, of which exons 3–6 correspond to the coding region of a 701-amino-acid protein [Laporte et al., 1997]. RT-PCR analysis of human cDNA samples detected the expression

M.I. and Y.W. contributed equally to this work.

1661–5425/15/0093–0130$39.50/0

E-Mail karger@karger.com
www.karger.com/sxd

Maki Fukami
Department of Molecular Endocrinology
National Research Institute for Child Health and Development
2-10-1 Ohkura, Setagaya, Tokyo 157-8535 (Japan)
E-Mail fukami-m@ncchd.go.jp

of full-length *MAMLD1* and its in-frame splice variant lacking exon 4 (Δexon 4) in all tissues examined [Fukami et al., 2006]. All essential domains of the MAMLD1 protein appear to be encoded by the sequences in exon 3, because the Δexon 4 variant retains normal transactivation activity for the *Hes3* promoter [Fukami et al., 2008], and a boy carrying a microdeletion involving exons 5–7 of *MAMLD1* had normal external genitalia [Tsai et al., 2005].

To date, several nucleotide alterations in *MAMLD1* have been identified in patients with hypospadias as well as in unaffected individuals [Fukami et al., 2006, 2008; Kalfa et al., 2008, 2011, 2012; Chen et al., 2010; Metwalley and Farghaly, 2012]. Of these, 4 nonsense [p.S70X (formerly p.S143X), p.E124X, p.Q197X, and p.R653X], 1 frameshift [p.E109fsX121 (formerly c.325delG)], and 2 missense substitutions [p.P311L (formerly p.P384L) and p.Q529K] have been identified exclusively in DSD patients and are therefore regarded as pathogenic mutations. In vitro assays using a luciferase reporter vector containing the *Hes3* promoter (pHes3-luc) indicated that p.S70X, p.E124X, p.Q197X, and p.P311L encode amorphic or hypomorphic proteins [Fukami et al., 2008; Kalfa et al., 2012]. The transactivation activities of the proteins encoded by p.E109fsX121 and p.Q529K have yet to be examined. Although p.R653X encodes a protein with normal transactivation activity, the mRNA transcript carrying this mutation is degraded through nonsense-mediated mRNA decay (NMD) [Fukami et al., 2008]. Similarly, p.S70X, p.E124X, p.Q197X, and p.E109fsX121 satisfy the condition for NMD [Kuzmiak and Maquat, 2006]. Taken together, all hypospadias-associated *MAMLD1* mutations reported to date are likely to generate dysfunctional proteins and/or unstable mRNAs.

Mutations in human genes exert pathogenic effects not only through generation of amorphic/hypomorphic proteins or unstable mRNAs, but also through several other mechanisms such as splicing defects, early protein degradation, and translation failure [Kuzmiak and Maquat, 2006; Bartoszewski et al., 2010; Ward and Cooper, 2010; Lee et al., 2011; Strachan and Read, 2011]. In particular, early protein degradation mediated by the proteasome or autophagy has been implicated in several genetic disorders [Kuroha et al., 2009; Strachan and Read, 2011; Ihara et al., 2012]. In the present study, we investigated the disease-causing mechanism associated with a novel mutation in *MAMLD1*.

Materials and Methods

Primers and Plasmid Vectors

Primers used in this study are shown in online supplementary table 1 (see www.karger.com/doi/10.1159/000380842 for all online suppl. material). The expression vector for the myc-tagged full-length wild-type MAMLD1 was created by inserting a cDNA fragment comprising 2,103 nucleotides of the coding region and 1,132 nucleotides of the 3′ untranslated region into a pCMV-Myc vector (Takara Bio, Ohtsu, Japan). Expression vectors for the mutant/variant MAMLD1 were created by site-directed mutagenesis (Takara Bio). The pHes3-luc reporter vector was kindly provided by Professor Kageyama.

Mutation Analysis of MAMLD1

This study was approved by the Institutional Review Board Committee at the National Center for Child Health and Development and performed after obtaining written informed consent. Mutation analysis of *MAMLD1* was performed for 180 patients with hypospadias. All patients had a 46,XY karyotype. Genomic DNA was extracted from peripheral leukocytes and amplified by PCR for coding exons 3–6 and their flanking splice sites of *MAMLD1*. The PCR products were subjected to direct sequencing.

mRNA and Protein Expression Analyses of Genital Skin Samples

A genital skin sample was obtained from a patient with a *MAMLD1* mutation during surgery for hypospadias. Control skin samples were obtained from 3 individuals with normal *MAMLD1* who underwent surgery for buried penis. Total RNAs and protein extracts were obtained from homogenized tissue samples. RT-PCR was performed using primers on exons 3 and 6 of *MAMLD1*. The PCR products were subcloned into the TOPO TA cloning vector (Life Technologies, Carlsbad, Calif., USA) and subjected to direct sequencing. PCR was also performed using primers specific for each splice variant. The products were analyzed by polyacrylamide gel electrophoresis using TBE-PAGE mini kit (TEFCO, Tokyo, Japan).

Western blot was carried out using anti-MAMLD1 antibodies (ab49150, Abcam, Cambridge, Mass., USA; and sc-131477, Santa Cruz Biotechnology, Calif., USA). Protein extracts were subjected to standard SDS-PAGE. The signals were visualized using BCIP/NBT Color Development Substrate (Promega, Madison, Wis., USA) or ECL Prime Western Blot Detection kit (GE Healthcare, Buckinghamshire, UK).

In vitro Protein Expression Assays

HEK293 cells were seeded in 10-cm plates (3.0×10^6 cells/plate) and transiently transfected using Lipofectamine 2000 (Life Technologies) with 10 μg of the expression vectors for the full-length wild-type or mutant/variant MAMLD1. The cells were harvested 48 h after transfection and the lysates were subjected to standard SDS-PAGE. The signals for the MAMLD1 proteins and the internal controls were probed with an anti-myc-tag antibody (Takara Bio) and an anti-β-actin antibody (Abcam), respectively. The relative expression levels of MAMLD1 proteins were calculated by dividing the signal intensities of the myc-tag by those of the internal control. Each experiment was performed in triplicate and repeated 3 times.

To clarify whether mutant MAMLD1 protein underwent early degradation, we performed further experiments using HEK293 cells seeded in 6-cm plates (1.0×10^6 cells/plate) and transfected

with 5 μg expression vectors. The transfected cells were treated with MG132, which inhibits proteasome-mediated degradation [Zhang et al., 2013]. In this experiment, MG132 (Peptide Institute, Osaka, Japan; final concentration, 50 μmol/l) was added to the medium 48 h after transfection, and the cells were cultured for further 1, 2, or 4 h. The transfected cells were also treated with cycloheximide (CHX), which inhibits both NMD and translation [Freddi et al., 2000]. CHX (Sigma-Aldrich, St. Louis, Mo., USA; final concentration, 100 μg/ml) was added to the medium 24 h after transfection, and the cells were cultured for further 24 or 48 h. The cells were harvested, and the lysates were subjected to Western blot analysis as mentioned above. Each experiment was repeated at least 3 times.

In vitro Transactivation Analysis

Transactivation activities of the full-length wild-type and mutant/variant MAMLD1 proteins were examined by luciferase reporter assays. HEK293 cells were seeded in 6-well plates (1.5×10^5 cells/well) and transiently transfected with 0.2 μg of the expression vectors and 0.2 μg of the pHes3-luc vector, together with 3 ng of the internal control vector. Relative luciferase activity was measured 48 h after transfection by the Dual Luciferase Reporter Assay System (Promega), using a pRL-CMV vector (Takara Bio) as an internal control. In addition, the same assays were carried out using different quantities of the expression vectors; we adjusted the amount of each plasmid such that all MAMLD1 proteins showed similar expression levels relative to that of β-actin. In these experiments, protein expression levels were quantified by ImageJ (imagej.nih.gov/ij/). The relative expression levels were calculated by dividing the signal intensities of MAMLD1 by those of β-actin (online suppl. fig. 1). Specifically, 8, 200, and 100 ng of the vectors for the full-length wild-type, mutant, and variant proteins, respectively, were used for transfection. Each experiment was performed in triplicate and repeated 3 times.

Statistical Analysis

The results are expressed as the mean ± SD, and statistical significance was determined using the t test. p values <0.05 were considered significant.

Results

Mutation Analysis of MAMLD1

A hemizygous nucleotide substitution (g.IVS4−2A>G) was identified in a patient with hypospadias (fig. 1A). The g.IVS4−2A>G mutation affected the consensus sequence at the splice acceptor site in intron 4. No pathogenic mutations were identified in the remaining 179 patients. The mutation-positive patient presented with penoscrotal hypospadias (fig. 1B). He had no family history of hypospadias. Ultrasonography at 1 month of age delineated 2 testes, each 10 × 10 × 14 mm, in the scrotum. Endocrine evaluation at 2 years and 11 months of age showed age-appropriate levels of gonadotropins and testosterone (LH <0.5 IU/l; FSH 1.6 IU/l, and testosterone <0.17 nmol/l).

mRNA and Protein Expression Analyses of Genital Skin Samples

Representative results are shown in figure 1C. RT-PCR of the control samples yielded bands of 3 different sizes, which corresponded to the full-length transcript, the Δexon 4 variant, and a hitherto unreported variant lacking exon 5 (Δexon 5). The Δexon 5 variant was predicted to encode a protein of 991 amino acids (c.1822_2065del, p.Q608fsX992). The majority of PCR products of the patient's sample were found to be the full-length transcript or the Δexon 5 variant. Furthermore, 4 of 17 clones of the full-length transcript lacked the first 10 nucleotides of exon 5, while the remaining clones had wild-type sequences. The full-length transcript with the 10-bp deletion was predicted to encode an elongated protein of 1,069 amino acids (c.1822_1831delACTCATGTAG, p.K609fsX1070). RT-PCR using specific primers for each splice variant yielded almost similar amounts of the full-length transcript and the Δexon 5 variant for all samples, whereas the PCR product for the Δexon 4 variant was barely detectable in the patient's sample.

In the Western blot analysis, no clear signals of MAMLD1 protein were detected in the genital skin samples of the patient or control individuals (data not shown).

In vitro Protein Expression Assays

Western blot analysis of cells transiently transfected with expression vectors for full-length wild-type MAMLD1, the p.K609fsX1070 mutant and the Δexon 5 variant detected proteins of expected masses (fig. 2A). However, the relative amounts of the mutant and Δexon 5 variant proteins were significantly lower than that of the wild-type protein (21.0% and 59.4% of the amount of wild-type protein, respectively). The expression levels of the wild-type and mutant proteins showed parallel increases upon MG132 treatment, indicating that proteasome-mediated degradation was unlikely in this case (fig. 2B). Likewise, the expression of the wild-type and mutant proteins decreased at a similar rate upon CHX treatment, indicating normal stability of the mutant MAMLD1 protein (fig. 2C).

In vitro Transactivation Analysis

The cells expressing the mutant and the Δexon 5 variant proteins showed lower luciferase activities than the cells expressing the wild-type protein (fig. 3A). The mutant and Δexon 5 variant proteins exerted apparently normal transactivating function when their expression was adjusted to a level similar to that of the wild-type protein (fig. 3B).

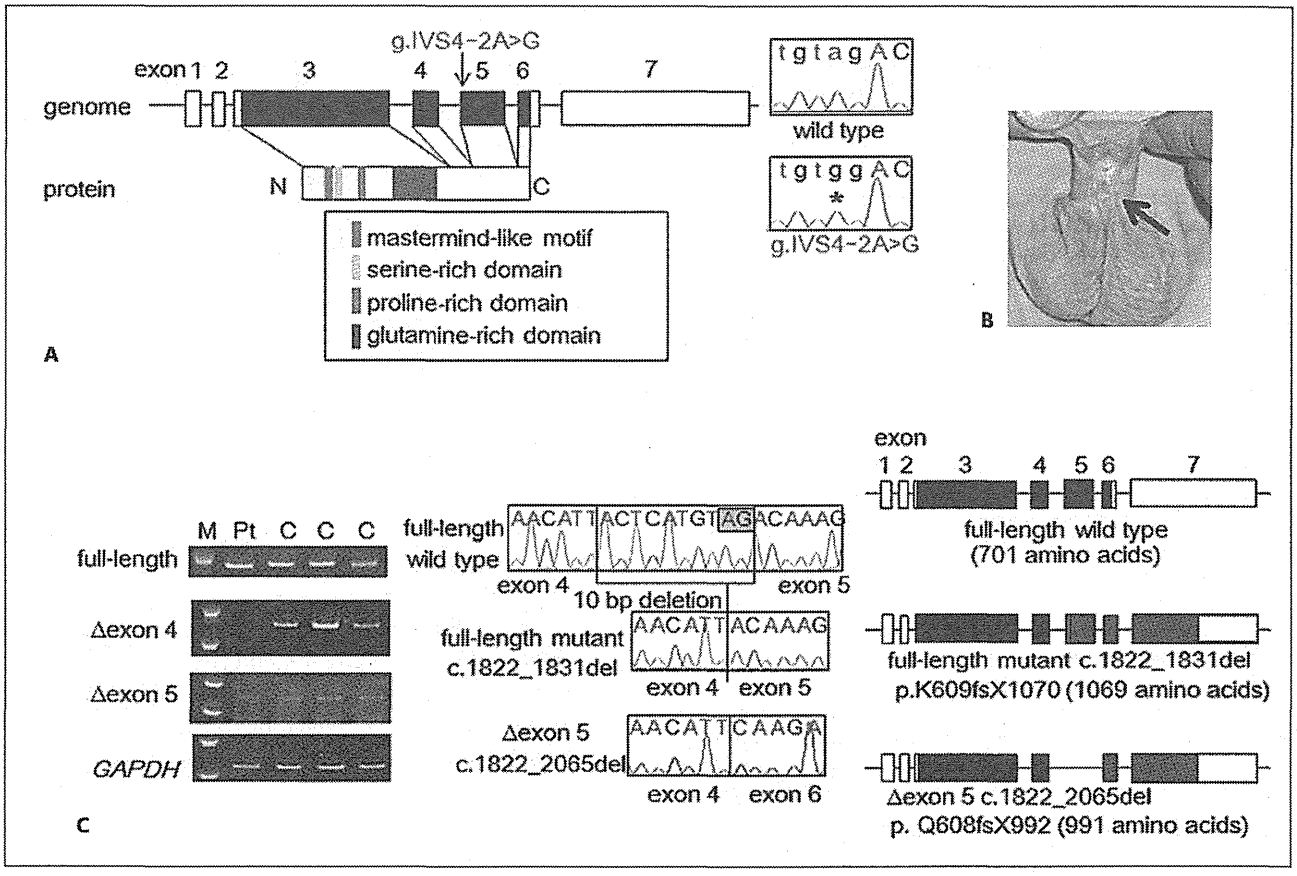

Fig. 1. *MAMLD1* mutation identified in the present study. **A** Position and sequence of the g.IVS4–2A>G mutation. The black and white boxes indicate the coding and non-coding regions, respectively. The asterisk depicts the mutated nucleotide. **B** Genital appearance of the mutation-positive patient. The arrow indicates the urethral meatus. **C** Representative results of the RT-PCR analysis of genital skin fibroblasts. Left panel: specific transcripts of *MAMLD1* splice variants. As an internal control, a house-keeping gene *(GAPDH)* was amplified. M = Molecular weight marker; C = control individuals; Pt = patient. Middle panel: the full-length transcript of the patient included the c.1822_1831del mutant. The 10-bp deletion can be ascribed to the activation of a cryptic splice acceptor site in exon 5 (shaded in red). Right panel: predicted protein structure of the transcripts. The black and white boxes indicate the coding and non-coding regions, respectively. The red box depicts the deleted region, and the blue boxes indicate aberrant amino acids encoded by frameshift mutation/variation.

Discussion

We identified a hemizygous intronic mutation in *MAMLD1* in 1 of 180 patients with hypospadias. These results support the previously proposed notion that *MAMLD1* mutations account for a small fraction of the etiology of hypospadias [Fukami et al., 2006]. RT-PCR of the patient's skin sample showed markedly reduced expression of the Δexon 4 variant and apparently normal expression of the full-length and Δexon 5 transcripts. Although the cause of the reduced expression of the Δexon 4 variant remains to be clarified, there are several examples of point mutations in human genes that alter the balance of splice variants [Sterne-Weiler et al., 2011; Ward and Cooper, 2010]. Disruption of a *cis*-acting splice enhancer or suppressor may underlie such a phenomenon [Sterne-Weiler et al., 2011]. Since the Δexon 4 variant of MAMLD1 is known to retain normal transactivation activity [Fukami et al., 2008], reduced expression of this variant may have played a role in the development of hypospadias in the patient.

Furthermore, the g.IVS4−2A>G mutation generated an mRNA lacking the first 10 nucleotides of exon 5. The 10-bp deletion can be explained by disruption of the

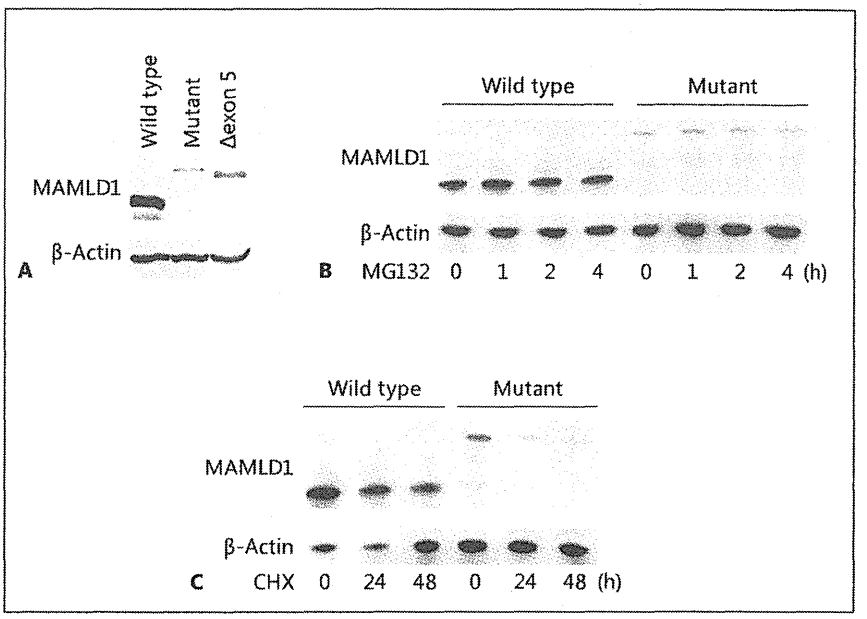

Fig. 2. Representative results of in vitro protein expression assays. **A** Western blot analysis of cells transiently transfected with the expression vectors for the full-length wild-type MAMLD1 (wild type), the p.K609fsX1070 mutant (mutant) and the Δexon 5 variant (Δexon 5). MAMLD1 proteins were probed with an anti-myc-tag antibody. β-Actin was analyzed as an internal control. **B**, **C** Effects of MG132, a proteasome inhibitor (**B**), and CHX, an inhibitor for translation and NMD (**C**), on MAMLD1 protein expression.

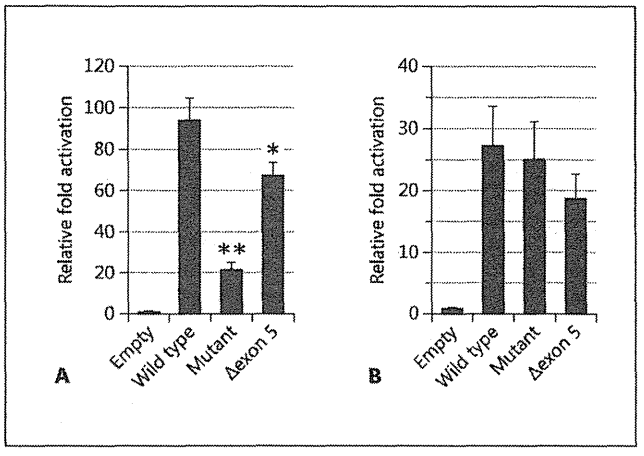

Fig. 3. Representative results of reporter assays. **A** Luciferase activities of cells transiently transfected with the expression vectors for the full-length wild-type MAMLD1 (wild type), the p.K609fsX1070 mutant (mutant) and the Δexon 5 variant (Δexon 5). Relative transactivation activity for the pHes3-luc reporter vector was measured. Significant differences are indicated by asterisks; * $p = 0.02$, ** $p = 0.0003$. **B** Luciferase activities of cells transfected with different amounts of expression vectors for the wild type, mutant and variant. The amount of each plasmid was adjusted such that all MAMLD1 proteins showed similar expression levels relative to that of β-actin. No significant difference was observed between the wild type and mutant or between the wild type and Δexon 5.

splice acceptor site in intron 4 and subsequent activation of the nearest cryptic splice site in exon 5 (fig. 1C). A substantial amount of the mutant mRNA was detected in the patient's cDNA, indicating that this transcript escapes NMD. On the other hand, in vitro assays revealed low expression levels of the mutant MAMLD1 protein. The cells expressing the mutant MAMLD1 showed markedly decreased luciferase activity of the Hes3-luc reporter, which was mostly ascribable to the reduced protein expression. Since the proteasome inhibitor MG132 and the translation inhibitor CHX exerted similar effects on the expression levels of the mutant and wild-type proteins in cultured cells, the g.IVS4−2A>G mutation is more likely to result in translation failure than in protein instability. Nevertheless, it remains unknown whether the expression of MAMLD1 protein is actually decreased in the mutation-positive patient. Western blot analysis did not show clear signals of MAMLD1 in genital skin tissues of the patient or control individuals. These findings may reflect the low expression of MAMLD1 in genital skin and/or the low binding specificity of the anti-MAMLD1 antibodies used in this study. In this regard, it is known that murine *Mamld1* is strongly expressed in fetal testis, but only weakly expressed in extragenital tissues [Fukami et al., 2006]. Thus, further studies, such as Western blot analyses of fetal testes of mutation-induced mice, are required to clarify the precise effect of this mutation.

The cells expressing the g.IVS4−2A>G mutation exhibited normal transactivating activity for the *Hes3* promoter after adjusting for protein expression levels. This suggests that the mutant MAMLD1 retains normal in vitro function. Nevertheless, we cannot exclude the possibility that the g.IVS4−2A>G mutation impairs in vivo function of MAMLD1, because there may be other target genes of MAMLD1 besides *HES3* [Fukami et al., 2008]. Indeed, a MAMLD1 missense variant p.P286S + p.N589S has been associated with the risk of hypospadias, although this variant retains normal in vitro transactivation activity for Hes3-luc [Kalfa et al., 2011].

Our patient manifested severe hypospadias in which the urethral opening was located at the penoscrotal region. Consistent with this, previously reported patients with pathogenic *MAMLD1* mutations invariably manifested severe hypospadias, except for 1 patient with a p.E109fsX121 mutation who presented with moderate hypospadias [Fukami et al., 2006, 2008; Kalfa et al., 2008, 2012; Chen et al., 2010; Metwalley and Farghaly, 2012]. These data imply that partial impairment of MAMLD1 function would be sufficient to cause severe hypospadias.

In conclusion, the results of the present study, in conjunction with those of previous investigations [Fukami et al., 2006, 2008; Kalfa et al., 2008, 2011, 2012; Chen et al., 2010; Metwalley and Farghaly, 2012], imply that various pathogenic events, including NMD, protein dysfunction and splicing errors, arise from *MAMLD1* mutations. Further analyses are necessary to clarify whether *MAMLD1* mutations can cause translation failure in vivo.

Acknowledgements

We thank Professor R. Kageyama for providing the pHes3-luc vector. This work was supported by the Grant-in-Aid for Young Scientists (B) from the Japan Society for the Promotion of Science; by the Grant-in-Aid for Scientific Research on Innovative Areas from the Ministry of Education, Culture, Sports, Science and Technology; by the Grant for Research on Intractable Diseases from the Ministry of Health, Labor and Welfare; by the Grants from the National Center for Child Health and Development, and from Takeda Foundation.

References

Bartoszewski RA, Jablonsky M, Bartoszewska S, Stevenson L, Dai Q, et al: A synonymous single nucleotide polymorphism in DeltaF508 CFTR alters the secondary structure of the mRNA and the expression of the mutant protein. J Biol Chem 285:28741–28748 (2010).

Chen Y, Thai HT, Lundin J, Lagerstedt-Robinson K, Zhao S, et al: Mutational study of the *MAMLD1*-gene in hypospadias. Eur J Med Genet 53:122–126 (2010).

Freddi S, Savarirayan R, Bateman JF: Molecular diagnosis of Stickler syndrome: a *COL2A1* stop codon mutation screening strategy that is not compromised by mutant mRNA instability. Am J Med Genet 90:398–406 (2000).

Fukami M, Wada Y, Miyabayashi K, Nishino I, Hasegawa T, et al: *CXorf6* is a causative gene for hypospadias. Nat Genet 38:1369–1371 (2006).

Fukami M, Wada Y, Okada M, Kato F, Katsumata N, et al: Mastermind-like domain-containing 1 (*MAMLD1* or *CXorf6*) transactivates the *Hes3* promoter, augments testosterone production, and contains the SF1 target sequence. J Biol Chem 283:5525–5532 (2008).

Ihara Y, Morishima-Kawashima M, Nixon R: The ubiquitin-proteasome system and the autophagic-lysosomal system in Alzheimer disease. Cold Spring Harb Perspect Med 2 pii: a006361 (2012).

Kalfa N, Liu B, Klein O, Audran F, Wang MH, et al: Mutations of *CXorf6* are associated with a range of severities of hypospadias. Eur J Endocrinol 159:453–458 (2008).

Kalfa N, Cassorla F, Audran F, Oulad Abdennabi I, Philibert P, et al: Polymorphisms of *MAMLD1* gene in hypospadias. J Pediatr Urol 7:585–591 (2011).

Kalfa N, Fukami M, Philibert P, Audran F, Pienkowski C, et al: Screening of *MAMLD1* mutations in 70 children with 46,XY DSD: identification and functional analysis of two new mutations. PLoS One 7:e32505 (2012).

Kuroha K, Tatematsu T, Inada T: Upf1 stimulates degradation of the product derived from aberrant messenger RNA containing a specific nonsense mutation by the proteasome. EMBO Rep 10:1265–1271 (2009).

Kuzmiak HA, Maquat LE: Applying nonsense-mediated mRNA decay research to the clinic: progress and challenges. Trends Mol Med 12: 306–316 (2006).

Laporte J, Kioschis P, Hu LJ, Kretz C, Carlsson B, et al: Cloning and characterization of an alternatively spliced gene in proximal Xq28 deleted in two patients with intersexual genitalia and myotubular myopathy. Genomics 41: 458–462 (1997).

Lee SM, Olzmann JA, Chin LS, Li L: Mutations associated with Charcot-Marie-Tooth disease cause SIMPLE protein mislocalization and degradation by the proteasome and aggresome-autophagy pathways. J Cell Sci 124: 3319–3331 (2011).

Metwalley KA, Farghaly HS: X-linked congenital adrenal hypoplasia associated with hypospadias in an Egyptian baby: a case report. J Med Case Rep 6:428 (2012).

Miyado M, Nakamura M, Miyado K, Morohashi K, Sano S, et al: MAMLD1 deficiency significantly reduces mRNA expression levels of multiple genes expressed in mouse fetal Leydig cells but permits normal genital and reproductive development. Endocrinology 153: 6033–6040 (2012).

Sterne-Weiler T, Howard J, Mort M, Cooper DN, Sanford JR: Loss of exon identity is a common mechanism of human inherited disease. Genome Res 21:1563–1571 (2011).

Strachan T, Read AP: Human genetic variability and its consequences, in Human Molecular Genetics, ed 4 (Garland Science, New York 2011).

Tsai TC, Horinouchi H, Noguchi S, Minami N, Murayama K, et al: Characterization of *MTM1* mutations in 31 Japanese families with myotubular myopathy, including a patient carrying 240 kb deletion in Xq28 without male hypogenitalism. Neuromuscul Disord 15:245–252 (2005).

Ward AJ, Cooper TA: The pathobiology of splicing. J Pathol 220:152–163 (2010).

Zhang WG, Souri M, Ichinose A: Proteosomal degradation of naturally recurring R260C missense and exon-IV deletion mutants of factor XIII A-subunit expressed in mammalian cells. Haemophilia 19:415–419 (2013).

Case Report

Cytogenetic and Genome Research

Cytogenet Genome Res 2014;144:285–289
DOI: 10.1159/000377649

Accepted: January 26, 2015
by M. Schmid
Published online: March 6, 2015

Microhomology-Mediated Microduplication in the Y Chromosomal Azoospermia Factor a Region in a Male with Mild Asthenozoospermia

Momori Katsumi[a] Hiromichi Ishikawa[d] Yoko Tanaka[e] Kazuki Saito[a, c]
Yoshitomo Kobori[f] Hiroshi Okada[f] Hidekazu Saito[c] Kazuhiko Nakabayashi[b]
Yoichi Matsubara[h] Tsutomu Ogata[a, g] Maki Fukami[a] Mami Miyado[a]

Departments of [a]Molecular Endocrinology and [b]Maternal-Fetal Biology, National Research Institute for Child Health and Development, and [c]Division of Reproductive Medicine, Center for Maternal-Fetal-Neonatal and Reproductive Medicine, National Medical Center for Children and Mothers, Tokyo, [d]Reproduction Center and [e]Department of Pediatrics, Tokyo Dental College Ichikawa General Hospital, Ichikawa, [f]Department of Urology, Dokkyo Medical University Koshigaya Hospital, Koshigaya, [g]Department of Pediatrics, Hamamatsu University School of Medicine, Hamamatsu, and [h]National Research Institute for Child Health and Development, Tokyo, Japan

Key Words
Azoospermia factor · Copy number variation · Duplication · Microhomology-mediated break-induced replication · Sperm motility

Abstract
Y chromosomal azoospermia factor (AZF) regions AZFa, AZFb and AZFc represent hotspots for copy number variations (CNVs) in the human genome; yet the number of reports of AZFa-linked duplications remains limited. Nonallelic homologous recombination has been proposed as the underlying mechanism of CNVs in AZF regions. In this study, we identified a hitherto unreported microduplication in the AZFa region in a Japanese male individual. The 629,812-bp duplication contained 22 of 46 exons of *USP9Y*, encoding the putative fine tuner of spermatogenesis, together with all exons of 3 other genes/pseudogenes. The breakpoints of the duplication resided in the DNA/TcMar-Tigger repeat and nonrepeat sequences, respectively, and were associated with a 2-bp microhomology, but not with short nucleotide stretches. The breakpoint-flanking regions were not enriched with GC content, palindromes, or noncanonical DNA structures. Semen analysis of the individual revealed a normal sperm concentration and mildly reduced sperm motility. The paternal DNA sample of the individual was not available for genetic analysis. The results indicate that CNVs in AZF regions can be generated by microhomology-mediated break-induced replication in the absence of known rearrangement-inducing DNA features. AZFa-linked microduplications likely permit production of a normal amount of sperm, although the precise clinical consequences of these CNVs await further investigation.

The long arm of the Y chromosome contains the azoospermia factor (AZF) regions AZFa, AZFb and AZFc that represent hotspots of copy number variations (CNVs) in the human genome [Vogt et al., 1996; Jobling, 2008; Krausz et al., 2011]. The high frequency of CNVs in AZF regions have been ascribed to the presence of multiple lo-

KARGER

E-Mail karger@karger.com
www.karger.com/cgr

1424–8581/15/1444–0285$39.50/0

Maki Fukami
Department of Molecular Endocrinology
National Research Institute for Child Health and Development
2-10-1 Ohkura, Tokyo 157-8535 (Japan)
E-Mail fukami-m@ncchd.go.jp

cus-specific repeats that serve as substrates for nonallelic homologous recombination (NAHR) [Repping et al., 2002; Vogt, 2005]. For example, NAHR between 2 human endogenous retroviral sequences underlies CNVs in the AZFa region [Kamp et al., 2000; Sun et al., 2000; Bosch and Jobling, 2003]. CNVs in the human genome are known to be caused not only by NAHR but also by microhomology-mediated break-induced replication (MMBIR) and nonhomologous end joining (NHEJ) [Gu et al., 2008; Hastings et al., 2009; van Binsbergen, 2011]. MMBIR and NHEJ produce CNVs whose fusion junctions are accompanied by microhomologies and short nucleotide stretches, respectively [Hastings et al., 2009; Ottaviani et al., 2014]. However, MMBIR and NHEJ have not yet been implicated in the development of AZF-linked CNVs, although Costa et al. [2008] proposed nonhomologous recombination as a possible mechanism of some microdeletions in the AZFb and AZFc regions. Furthermore, it remains unknown whether AZF-linked CNVs are triggered by known rearrangement-inducing DNA features, such as high GC content, palindromes, and noncanonical DNA structures [Kurahashi et al., 2006; Gu et al., 2008; Cooper et al., 2011; Froyen et al., 2012].

Deletions and duplications in the AZFb and AZFc regions frequently result in oligo/azoospermia and asthenozoospermia [Repping et al., 2002; Eloualid et al., 2012; Rozen et al., 2012], while deletions in the AZFa region lead to complete germ cell aplasia [Kamp et al., 2000]. AZF-linked deletions were found in about 7% of infertile men [Simoni et al., 1999]. In contrast, duplications in the AZFa region were suggested to be compatible with male fertility [Bosch and Jobling, 2003; Arruda et al., 2008]. However, since there have been only 2 reports of duplications in the AZFa region, the functional neutrality of such CNVs remains rather speculative. Here, we present a hitherto unreported microduplication in the AZFa region identified in a male individual with mild asthenozoospermia.

Case Report

Patient

A 37-year-old Japanese man visited our clinic because of infertility after 4 years of regular intercourse. He manifested no additional clinical features. His stature was 177 cm (+0.96 SD). He had normal pubic and axillary hair, and his testicular volumes were within the normal range (right, 14 ml; left, 16 ml). His semen samples were obtained by masturbation after 5 days of abstinence, kept at room temperature, and analyzed within a few hours after collection. Motility was assessed directly after liquefaction. The semen parameters were assessed according to the WHO laboratory manual (4th edition). As a result, a normal sperm concentration and mildly decreased sperm motility were observed in 2 independent samples (table 1). Endocrine examinations revealed normal blood levels of LH (2.0 mIU/ml; reference range, 1.0–8.4 mIU/ml), FSH (8.6 mIU/ml; reference range, 1.0–10.5 mIU/ml), prolactin (6.4 ng/ml; reference range, 1.5–9.7 ng/ml), and testosterone (4.0 ng/ml; reference range, 2.5–11.0 ng/ml). His karyotype was 46,XY. He was diagnosed with mild asthenozoospermia and subjected to copy number analysis of AZF regions.

Table 1. Semen findings of the patient

	Samples		Reference range[a]
	first	second	
Ejaculate volume, ml	3.2	4.4	>1.5
Sperm concentration, $\times 10^6$/ml	49	23	>15
Total motility, %	16.3	21.7	>40.0
Normal morphology, %	6.1	5.7	>4.0

[a] Based on WHO data.

Molecular Analyses

This study was approved by the Institutional Review Board Committee at the National Center for Child Health and Development. After taking written informed consent, a genomic DNA sample was obtained from the patient. We also attempted to obtain DNA samples from the patient's parents. CNVs in the AZF regions were analyzed by multiplex ligation-dependent probe amplification (MLPA) (SALSA MLPA probe-mix kit P360-A1, MRC-Holland, Amsterdam, the Netherlands). A CNV identified by MLPA was further characterized by array-based comparative genomic hybridization (CGH) using a human catalog array (8 × 60 k format, Agilent technologies, Palo Alto, Calif., USA). We also investigated the presence or absence of additional CNVs in the Y chromosome. CNVs were called using the Genomic Workbench Software (version 7.0.4.0) with the default settings of the aberration detection algorithm (ADM-2; Agilent Technologies). The fusion junction of the AZF-linked CNV was determined by long-range PCR using serial primers that hybridized to the breakpoint-flanking regions (fig. 1c; online suppl. table 1, for all online suppl. material, see www.karger.com/doi/10.1159/000377649). To clarify whether the breakpoints of the CNV were associated with repeat sequences or known rearrangement-inducing DNA features, we analyzed 150-bp regions around the breakpoints using RepeatMasker (http://www.repeatmasker.org), geecee (http://emboss.bioinformatics.nl/cgi-bin/emboss/geecee), palindrome (http://mobyle.pasteur.fr/cgi-bin/portal.py#forms::palindrome), and non-B DB (http://nonb.abcc.ncifcrf.gov).

Results

MLPA showed increased relative peak areas of 5 probes for a genomic locus in the AZFa region (fig. 1a). CGH confirmed a copy number gain of a ~0.6-Mb genomic interval in the AZFa region and excluded the presence of other

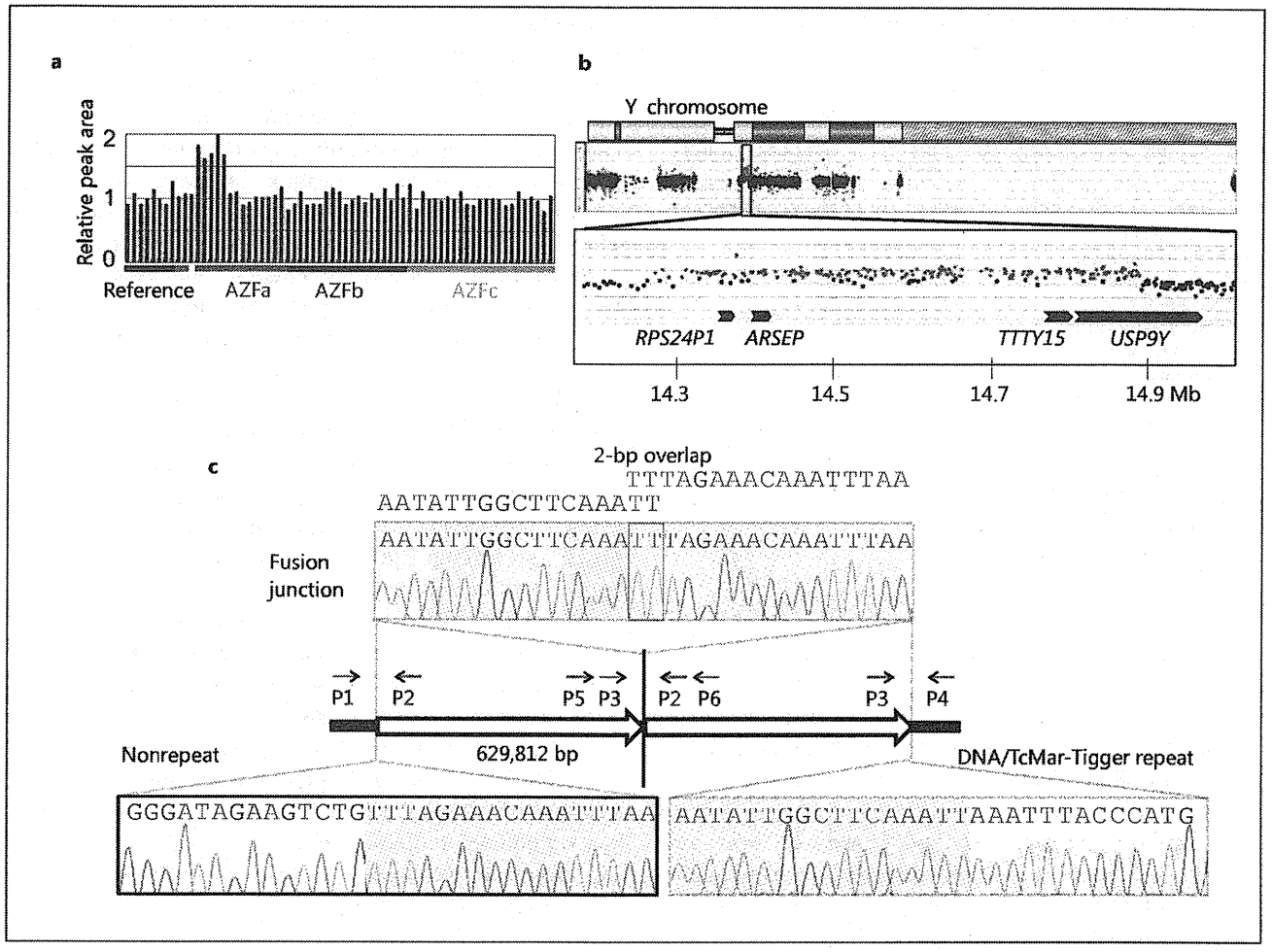

Fig. 1. The CNV in the AZFa region. **a** MLPA. Increased relative peak areas (>1.5) of 5 probes indicate a copy number gain of the corresponding loci. The relative peak area of each probe was calculated by dividing the actual peak area of the subject by the average of the areas of 5 reference samples. **b** CGH. The black, red, and green dots denote signals indicative of the normal, increased (>+0.4), and decreased (<–0.8) copy numbers, respectively. Genomic positions refer to Human Genome Database (hg19, build 37). All positive signals except for those in the AZFa region were not assessed as CNVs. **c** Schematic representation of the rearrangement and the DNA sequences at the fusion junction. P1–P6 indicate PCR primers shown in online supplementary table 1.

CNVs in the Y chromosome (fig. 1b). Although CGH yielded signals that were indicative of CNVs in several Y chromosomal regions, all positive signals except for those in the AZFa region were not assessed as CNVs. Characterization of the fusion junction indicated that the CNV in the AZFa region was a simple tandem duplication of 629,812 bp (chrY:14,264,798–14,894,609; hg19, build 37) (fig. 1c; online suppl. fig. 1). This duplication encompassed 22 of 46 exons of *USP9Y* (accession number NM_004654), together with all exons of *TTTY15* (NR_001545) and 2 pseudogenes *RPS24P1* (NG_000893) and *ARSEP* (NG_000880). The telomeric breakpoint of the duplication was located within the DNA/TcMar-Tigger repeat, while the centromeric breakpoint resided in a nonrepeat sequence (fig. 1c). The breakpoints had no long-sequence similarity, but shared microhomology of 2 bp. Nucleotide stretches were not observed at the fusion junction. In silico analysis showed that the breakpoint-flanking regions were not enriched with GC content or palindromes and that only one of the 4 regions contained multiple noncanonical DNA structures (table 2). Parental DNA samples of the patient were not available for molecular analysis.

Table 2. In silico analyses of the breakpoint-flanking regions

	Breakpoints			
	centromeric		telomeric	
Genomic position	14,264,647–14,264,797	14,264,797–14,264,947	14,894,458–14,894,608	14,894,608–14,894,758
GC content[a]	32%	38%	39%	40%
Palindrome ≥10 bp	0	0	0	0
Noncanonical structure				
A-phased repeat	0	0	0	0
Direct repeat	0	2	0	0
G-quadruplex motif	0	0	0	0
Inverted repeat	1	1	0	1
Mirror repeat	0	2	0	0
Short tandem repeat	0	2	0	0
Z-DNA motif	0	2	0	0

Genomic positions are referred to Human Genome Database (hg19, build 37). [a] Average GC content in the human genome is ~40% [Li, 2011].

Discussion

We identified a tandem microduplication involving a ~0.6-Mb genomic interval of the AZFa region in a male individual. Telomeric and centromeric breakpoints of the duplication resided in repeat and nonrepeat sequences, respectively, and shared a 2-bp microhomology. The fusion junction was not accompanied by short nucleotide stretches. Collectively, these findings suggest MMBIR as the underlying mechanism of the duplication. The breakpoint-flanking regions of the present case were not enriched with known rearrangement-inducing DNA features, indicating that hitherto unknown genomic motifs may play a role in the development of this duplication. To our knowledge, this is the first example of AZF-linked CNVs generated by replication-based mechanisms. In this context, recent studies have shown that MMBIR is involved in several simple and complex rearrangements in the human genome [Zhang et al., 2009; van Binsbergen, 2011; Ottaviani et al., 2014]. Thus, it is possible that MMBIR represents a rare etiology of AZF-linked CNVs. MMBIR-mediated CNVs may be more common in the AZFa region than in the AZFb/c regions because the AZFa region contains less long repeats that could lead to NAHR [Gu et al., 2008; Jobling, 2008].

Clinical analyses of our patient suggested that the ~0.6-Mb duplication permits production of a normal amount of sperm. On the other hand, the association between the duplication and asthenozoospermia in this patient remains uncertain. Notably, the telomeric breakpoint of this duplication was located at intron 22 of *USP9Y*. Since the USP9Y protein is predicted to act as a fine tuner of the human spermatogenic process [Krausz et al., 2006], disruption of one copy of this gene may exert a negative effect on sperm motility. However, it is possible that the duplication is a functionally neutral polymorphism. If this is the case, asthenozoospermia of the patient would be ascribed to other genetic or environmental factors. Furthermore, we cannot exclude the possibility that the mildly impaired sperm motility of the patient is a laboratory artifact. Since the paternal DNA sample of the patient was not available for molecular analysis, it remains unknown whether the duplication is shared by the fertile father. In this regard, previous studies suggested that ~0.8-Mb duplications encompassing the major part of the AZFa region are compatible with male fertility [Bosch and Jobling, 2003; Arruda et al., 2008], although sperm motility was not evaluated in the previously reported microduplication-positive individuals. Thus, further studies are necessary to clarify whether asthenozoospermia is a consistent feature in individuals with microduplications in the AZFa region.

In conclusion, we identified a hitherto unreported microduplication in the AZFa region. This duplication appeared to be caused by MMBIR in the absence of known rearrangement-inducing DNA features. Further studies are necessary to clarify the clinical consequences of AZFa-linked duplications.

Acknowledgements

This work is supported by Grants-in-Aid from the Ministry of Education, Culture, Sports, Science and Technology, from the Japan Society for the Promotion of Science and by Grants from the Ministry of Health, Labor and Welfare, from the National Center for Child Health and Development, and from the Takeda Science Foundation.

References

Arruda JT, Silva DM, Silva CC, Moura KK, da Cruz AD: Homologous recombination between HERVs causes duplications in the AZFa region of men accidentally exposed to cesium-137 in Goiânia. Genet Mol Res 7: 1063–1069 (2008).

Bosch E, Jobling MA: Duplications of the AZFa region of the human Y chromosome are mediated by homologous recombination between HERVs and are compatible with male fertility. Hum Mol Genet 12:341–347 (2003).

Cooper DN, Bacolla A, Férec C, Vasquez KM, Kehrer-Sawatzki H, Chen JM: On the sequence-directed nature of human gene mutation: the role of genomic architecture and the local DNA sequence environment in mediating gene mutations underlying human inherited disease. Hum Mutat 32:1075–1099 (2011).

Costa P, Gonçalves R, Ferrás C, Fernandes S, Fernandes AT, et al: Identification of new breakpoints in AZFb and AZFc. Mol Hum Reprod 14:251–258 (2008).

Eloualid A, Rhaissi H, Reguig A, Bounaceur S, El Houate B, et al: Association of spermatogenic failure with the b2/b3 partial AZFc deletion. PLoS One 7:e34902 (2012).

Froyen G, Belet S, Martinez F, Santos-Rebouças CB, Declercq M, et al: Copy-number gains of *HUWE1* due to replication- and recombination-based rearrangements. Am J Hum Genet 91:252–264 (2012).

Gu W, Zhang F, Lupski JR: Mechanisms for human genomic rearrangements. Pathogenetics 1:4 (2008).

Hastings PJ, Ira G, Lupski JR: A microhomology-mediated break-induced replication model for the origin of human copy number variation. PLoS Genet 5:e1000327 (2009).

Jobling MA: Copy number variation on the human Y chromosome. Cytogenet Genome Res 123:253–262 (2008).

Kamp C, Hirschmann P, Voss H, Huellen K, Vogt PH: Two long homologous retroviral sequence blocks in proximal Yq11 cause AZFa microdeletions as a result of intrachromosomal recombination events. Hum Mol Genet 9:2563–2572 (2000).

Krausz C, Degl'Innocenti S, Nuti F, Morelli A, Felici F, et al: Natural transmission of *USP9Y* gene mutations: a new perspective on the role of *AZFa* genes in male fertility. Hum Mol Genet 15:2673–2681 (2006).

Krausz C, Chianese C, Giachini C, Guarducci E, Laface I, Forti G: The Y chromosome-linked copy number variations and male fertility. J Endocrinol Invest 34:376–382 (2011).

Kurahashi H, Inagaki H, Ohye T, Kogo H, Kato T, Emanuel BS: Palindrome-mediated chromosomal translocations in humans. DNA Repair (Amst) 5:1136–1145 (2006).

Li W: On parameters of the human genome. J Theor Biol 288:92–104 (2011).

Ottaviani D, LeCain M, Sheer D: The role of microhomology in genomic structural variation. Trends Genet 30:85–94 (2014).

Repping S, Skaletsky H, Lange J, Silber S, Van Der Veen F, et al: Recombination between palindromes P5 and P1 on the human Y chromosome causes massive deletions and spermatogenic failure. Am J Hum Genet 7:906–922 (2002).

Rozen SG, Marszalek JD, Irenze K, Skaletsky H, Brown LG, et al: *AZFc* deletions and spermatogenic failure: a population-based survey of 20,000 Y chromosomes. Am J Hum Genet 91:890–896 (2012).

Simoni M, Bakker E, Eurlings MC, Matthijs G, Moro E, et al: Laboratory guidelines for molecular diagnosis of Y-chromosomal microdeletions. Int J Androl 22:292–299 (1999).

Sun C, Skaletsky H, Rozen S, Gromoll J, Nieschlag E, et al: Deletion of azoospermia factor a *(AZFa)* region of human Y chromosome caused by recombination between HERV15 proviruses. Hum Mol Genet 9:2291–2296 (2000).

van Binsbergen E: Origins and breakpoint analyses of copy number variations: up close and personal. Cytogenet Genome Res 135:271–276 (2011).

Vogt PH: *AZF* deletions and Y chromosomal haplogroups: history and update based on sequence. Hum Reprod Update 11:319–336 (2005).

Vogt PH, Edelmann A, Kirsch S, Henegariu O, Hirschmann P, et al: Human Y chromosome azoospermia factors (AZF) mapped to different subregions in Yq11. Hum Mol Genet 5:933–943 (1996).

Zhang F, Carvalho CM, Lupski JR: Complex human chromosomal and genomic rearrangements. Trends Genet 25:298–307 (2009).

OPEN

Citation: Human Genome Variation (2015) 2, 15020; doi:10.1038/hgv.2015.20

www.nature.com/hgv

DATA REPORT

Endocrinopathies in a boy with cryptic copy-number variations on 4q, 7q and Xp

Misako Okuno[1,2], Tsutomu Ogata[1,3], Kazuhiko Nakabayashi[4], Tatsuhiko Urakami[2], Maki Fukami[1] and Keisuke Nagasaki[1,5]

We report a male patient with three copy-number variations (CNVs) and unique phenotype. He carried ~11.2 Mb terminal duplication on 4q, ~13.4 Mb terminal deletion on 7q and ~1.7 Mb interstitial duplication on Xp22.31, which were identified by array-based comparative genomic hybridization. He manifested mental retardation, mild brain anomalies and skeletal deformities ascribable to these CNVs, together with central precocious puberty and mild adrenocorticotropic hormone overproduction of unknown etiologies.

Human Genome Variation (2015) **2**, 15020; doi:10.1038/hgv.2015.20; published online 2 July 2015

Molecular cytogenetic technologies, including array-based comparative genomic hybridization, are useful to identify cryptic copy-number variations (CNVs) in individuals with an apparently normal karyotype.[1–3] Recent cytogenetic studies have shown that cryptic CNVs account for a certain fraction of the etiologies of congenital disorders.[1–3] Cryptic CNVs can underlie complex phenotypes that are not explainable by monogenic mutations, although they can also occur as benign polymorphisms.[2,3]

Here, we report a male patient with unique endocrine abnormalities and additional clinical features, in whom we identified three cryptic CNVs. This study was approved by the Institutional Review Board Committee at the National Center for Child Health and Development and performed after obtaining informed consent. The patient was born to non-consanguineous Japanese parents at 40 weeks of gestation. The patient's parents were clinically normal, whereas two sisters and two of three maternal uncles of the patient had mild mental retardation. Endocrinological assessments were not performed for the family members. At birth, the patient showed mild genital skin pigmentation, mild joint contractures and muscle hypertonia. He had no episodes of hypoglycemia or seizure. His mental development was markedly delayed. He started walking on his own at 6 years of age. At 8 years of age, he was referred to our hospital for the evaluation of early sexual maturation. Physical assessment showed pubic hair of Tanner stage 2, penis of stage 5 and bilateral testes of 8 ml (+9.1 s.d.). He manifested skin pigmentation in the external genitalia, gingiva and fingers. In addition, he showed scoliosis and restricted joint extension of the limbs. He had no facial dysmorphism, except for strabismus, a broad nasal base and platycephaly. He spoke multiple words but no sentences, and was unable to run. His height and weight were 118.2 cm (−1.6 s.d.) and 20.8 kg (−1.1 s.d.), respectively. He had a significantly advanced bone age (14 years and 1 month); his predicted final height was around 130 cm (−7.0 s.d.). Skeletal radiography showed Madelung-like deformity of the forearm and scoliosis. Brain magnetic resonance imaging detected mild ventricular dilatation and mild atrophy of the anterior lobe. No abnormalities were observed in the hypothalamus or pituitary. Abdominal ultrasonography and computed tomography showed no abnormalities. Endocrine assessment revealed an elevated testosterone level and increased gonadotropin responses to gonadotropin-releasing hormone stimulation, which collectively indicated central precocious puberty (Table 1). He showed a mildly elevated level of insulin-like growth factor 1, which was consistent with the accelerated sexual maturation.[4] Adrenocorticotropic hormone (ACTH) levels were elevated before and after corticotropin-releasing factor stimulation, while cortisol levels remained normal (Table 1). These data were consistent with a condition referred to as 'overproduction of ACTH, not associated with Cushing disease' (International Statistical Classification of Diseases and Related Health Problems 10th Revision). Blood levels of glucose and electrolytes were within the normal range. G-banding analysis showed a normal 46,XY karyotype. Array-based comparative genomic hybridization using a human catalog array (4×180 k format, Agilent Technologies, Santa Clara, CA, USA) delineated three heterozygous CNVs, i.e., ~11.2 Mb terminal duplication on 4q34.3-35.2, ~13.4 Mb terminal deletion on 7q35-36.3 and ~1.7 Mb interstitial duplication on Xp22.31 (Figure 1; Supplementary Table S1). These CNVs were not found in the database of Genomic Variants (http://dgv.tcag.ca/dgv/app/home?ref=GRCh37/hg19) or in the University of California Santa Cruz Genome Browser (https://genome.ucsc.edu/). The mother of the boy had the same duplication on Xp22.31, but no other CNV. DNA samples of other family members were not available for genetic testing.

These data suggest that the boy carried *de novo* or paternally inherited CNVs on 4q and 7q, and a maternally inherited duplication on Xp (Supplementary Table S1). CNVs on 4q and 7q appear to be pathogenic, because they affected more than 10 Mb regions and have been reported exclusively in individuals

[1]Department of Molecular Endocrinology, National Research Institute for Child Health and Development, Tokyo, Japan; [2]Department of Pediatrics, Nihon University School of Medicine, Tokyo, Japan; [3]Department of Pediatrics, Hamamatsu University School of Medicine, Hamamatsu, Japan; [4]Department of Maternal-Fetal Biology, National Research Institute for Child Health and Development, Tokyo, Japan and [5]Division of Pediatrics, Department of Homeostatic Regulation and Development, Niigata University Graduate School of Medical and Dental Sciences, Niigata, Japan.
Correspondence: M Fukami (fukami-m@ncchd.go.jp)
Received 11 March 2015; revised 1 April 2015; accepted 3 April 2015

Table 1. Endocrine findings of the patient at 8 years of age

Hormone	*Stimulus (dosage)*	*Patient*		*Reference values*[a]		*Coversion factor to the SI unit*
		Baseline	*Peak*	*Baseline*	*Peak*	
Growth hormone (ng/ml)	GRF (20 μg)[b]	1.3	35.1		>15	1.0 (μg/l)
Luteinizing hormone (mIU/ml)	GnRH (80 μg)[c]	2.8	61.8	0.0–0.4	0.4–6.0	1.0 (IU/l)
Follicle stimulating hormone (mIU/ml)	GnRH (80 μg)[c]	11.1	46.3	0.6–3.0	6.3–15.6	1.0 (IU/l)
Thyroid stimulating hormone (mIU/ml)	TRH (140 μg)[c]	2.3	24.5	0.2–5.4	3.6–26.8	1.0 (mIU/l)
Prolactin (ng/ml)	TRH (140 μg)[c]	7.1	31.5	1.4–11.8		43.48 (pmol/l)
Adrenocorticotropic hormone (pg/ml)	CRF (20 μg)[b]	158	486	10–25	28–131	0.22 (pmol/l)
Cortisol (μg/dl)	CRF (20 μg)[b]	9.1	15.4	6.1–12.3	10.6–26.9	27.59 (nmol/l)
Cortisol (μg/dl)	ACTH (0.2 mg)[d]	7.1	**18.5**	6.1–12.3	22.7–25.9	27.59 (nmol/l)
17α-Hydroxypregnenolone (ng/ml)	ACTH (0.2 mg)[d]	0.95	2.39	0.26–1.43	1.29–3.92	0.301 (pmol/l)
17-Hydroxyprogesterone (ng/ml)	ACTH (0.2 mg)[d]	0.4	1.8	0.2–0.5	1.1–1.8	0.303 (pmol/l)
Dehydroepiandrosterone sulfate (μg/dl)		12.1		4.41–24.4		0.02714 (μmol/l)
Insulin-like growth factor 1 (ng/ml)		240		114–225		0.131 (nmol/l)
Testosterone (ng/dl)		300		1–13		0.03467 (nmol/l)
Free triiodothyronine (pg/ml)		3.1		3.1–5.1		1.536 (pmol/l)
Free thyroxine (ng/dl)		1.1		1.1–1.6		0.1287 (pmol/l)

Abbreviations: ACTH, adrenocorticotropic hormone; CRF, corticotropin-releasing factor; GnRH, gonadotropin-releasing hormone; GRF, growth hormone releasing factor; TRH, thyrotropin-releasing hormone. Hormone values below the reference range are boldfaced and those above the reference range are underlined. Stimulus dosage was administered i.v. [a]Reference values in age-matched males. [b]Blood sampling at 0, 15, 30, 60, 90 and 120 min. [c]Blood sampling at 0, 30, 60, 90 and 120 min. [d]Blood sampling at 0, 30 and 60 min.

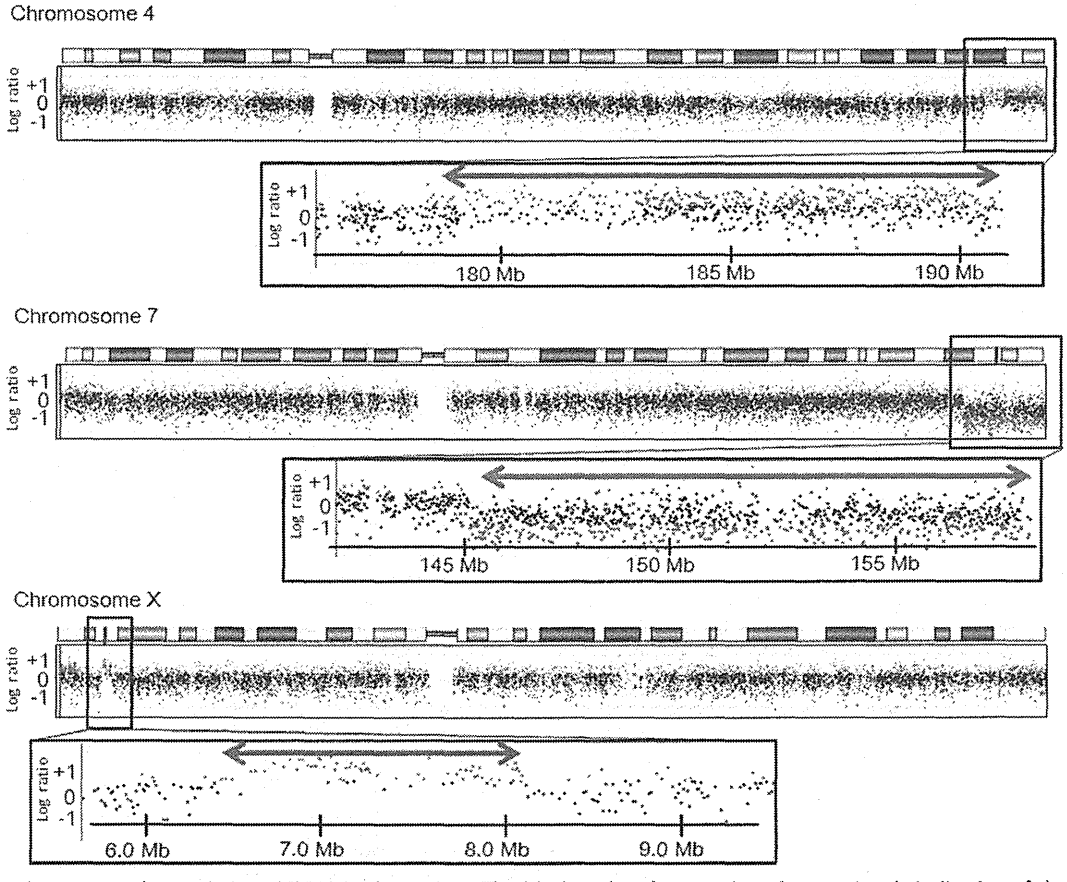

Figure 1. Cryptic copy-number variations (CNVs) in the patient. The black, red and green dots denote signals indicative of the normal, the increased (log ratio ≥ + 0.5) and the decreased (log ratio ≤ − 1.0) copy-numbers, respectively. Genomic positions correspond to the human genome reference assembly (UCSC Genome Browser, hg19, build 37). The red and green arrows indicate the duplicated and deleted regions, respectively. The names of the genes affected by the CNVs are shown in Supplementary Table S1.